

Measurement of the UH-60A Hub/Large Rotor Test Apparatus Control System Stiffness

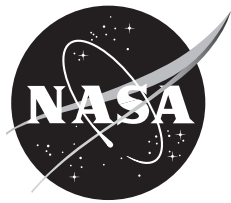
*Robert M. Kufeld
Ames Research Center
Moffett Field, California*

The NASA STI Program Office . . . in Profile

Since its founding, NASA has been dedicated to the advancement of aeronautics and space science. The NASA Scientific and Technical Information (STI) Program Office plays a key part in helping NASA maintain this important role.

The NASA STI Program Office is operated by Langley Research Center, the Lead Center for NASA's scientific and technical information. The NASA STI Program Office provides access to the NASA STI Database, the largest collection of aeronautical and space science STI in the world. The Program Office is also NASA's institutional mechanism for disseminating the results of its research and development activities. These results are published by NASA in the NASA STI Report Series, which includes the following report types:

- **CONFERENCE PUBLICATION.** Collected papers from scientific and technical conferences, symposia, seminars, or other meetings sponsored or cosponsored by NASA.
 - **SPECIAL PUBLICATION.** Scientific, technical, or historical information from NASA programs, projects, and missions, often concerned with subjects having substantial public interest.
 - **TECHNICAL TRANSLATION.** English-language translations of foreign scientific and technical material pertinent to NASA's mission.
- Specialized services that complement the STI Program Office's diverse offerings include creating custom thesauri, building customized databases, organizing and publishing research results . . . even providing videos.
- For more information about the NASA STI Program Office, see the following:
- Access the NASA STI Program Home Page at <http://www.sti.nasa.gov>
 - E-mail your question via the Internet to help@sti.nasa.gov
 - Fax your question to the NASA Access Help Desk at (301) 621-0134
 - Telephone the NASA Access Help Desk at (301) 621-0390
 - Write to:
NASA Access Help Desk
NASA Center for AeroSpace Information
7115 Standard Drive
Hanover, MD 21076-1320



Measurement of the UH-60A Hub/Large Rotor Test Apparatus Control System Stiffness

*Robert M. Kufeld
Ames Research Center
Moffett Field, California*

National Aeronautics and
Space Administration

Ames Research Center
Moffett Field, California 94035-1000

Available from:

NASA Center for AeroSpace Information
7115 Standard Drive
Hanover, MD 21076-1320
(301) 621-0390

National Technical Information Service
5285 Port Royal Road
Springfield, VA 22161
(703) 487-4650

TABLE OF CONTENTS

List of Figures	v
Nomenclature	vii
Summary	1
Introduction	1
Differences Between Aircraft and LRTA Control Systems	2
Control System Stiffness Measurement Technique	7
Setup	8
Testing Procedure	10
Results	13
Multi-blade Coordinate Transformations	19
Conclusion	21
References	22
Appendix	23

LIST OF FIGURES

Figure 1. UH-60A Airloads rotor mounted on the LRTA inside the NFAC 40- by 80-Foot Wind Tunnel	2
Figure 2. Schematic of the UH-60A and LRTA swashplate and stationary link locations.....	3
Figure 3. Cutaway view of UH-60A control system linkages.....	3
Figure 4. Primary actuator and rocker arm schematic.	5
Figure 5. Dynamic actuator schematic.....	5
Figure 6. Photograph of LRTA rocker arm and dynamic actuator.	6
Figure 7. Single stationary link for the forward and aft swashplate connection.....	6
Figure 8. Two-component stationary link for the lateral swashplate connection.	7
Figure 9. Schematic of control stiffness measurement hardware.....	9
Figure 10. Photo of UH-60A hub spindle with control stiffness measurement hardware installed.....	9
Figure 11. Detailed photo of the interface link passing through a rod end and connecting to the position encoder via a flexible coupling.	10
Figure 12. Time history measurement of blade 2 with dynamic actuators active and off: 270-degree azimuth, collective loading.....	11
Figure 13. Maximum collective loading condition, 250 pounds hanging from all four moment arms.....	13
Figure 14. Typical measurement results for blade spindle near the 90- or 270-degree azimuth position: blade 1, collective loading, 75-degree rotor azimuth, and dynamic actuators off, linear equation shown.	14
Figure 15. Typical measurement results for blade spindle near the 0-degree azimuth position: blade 2, collective loading, 345-degree rotor azimuth, and dynamic actuators off, linear equation shown.	15
Figure 16. Typical measurement results for blade spindle near the 180-degree azimuth position: blade 3, collective loading, 195-degree rotor azimuth, dynamic actuators active, and linear equation shown.	15
Figure 17. Typical measurement results for blade spindle under cyclic loading: blade 1, cyclic loading, 15-degree rotor azimuth, dynamic actuator off, linear equations for upper half of data and lower half of data.	16
Figure 18. Azimuthal variation of LRTA control stiffness for collective loading with the dynamic actuators active and off compared to UH-60A aircraft.....	17

LIST OF FIGURES (CONTINUED)

Figure 19. Azimuthal variation of LRTA control stiffness for reactionless loading with the dynamic actuators active and off compared to UH-60A aircraft.....	18
Figure 20. Azimuthal variation of LRTA control stiffness for cyclic loading with the dynamic actuators active and off compared to UH-60A aircraft.....	18
Figure 21. Diagonal elements of the fixed-system control stiffness as a function of the reference blade azimuth position for dynamic actuators off	20
Figure 22. Diagonal elements of the fixed-system control stiffness as a function of the reference blade azimuth position for dynamic actuators active.....	21

NOMENCLATURE

K Measured Control System Stiffness, ft-lb/deg

M Applied Moment, ft-lb

θ Spindle deflection, deg

ψ Rotor Blade Azimuth, deg

Subscripts

col Collective Loading

cos Cosine Cyclic Loading

sin Sine Cyclic Loading

react Reactionless Loading

MEASUREMENT OF THE UH-60A HUB / LARGE ROTOR TEST APPARATUS CONTROL SYSTEM STIFFNESS

Robert M. Kufeld

Ames Research Center

SUMMARY

This report provides details of the measurement of the control system stiffness of the UH-60A rotor hub mounted on the Large Rotor Test Apparatus (UH-60A/LRTA). The UH-60A/LRTA was used in the 40- by 80-Foot Wind Tunnel to complete the full-scale wind tunnel test portion of the NASA / ARMY UH-60A Airloads Program. This report describes the LRTA control system and highlights the differences between the LRTA and UH-60A aircraft. The test hardware, test setup, and test procedures are also described. Sample results are shown, including the azimuthal variation of the measured control system stiffness for three different loadings and two different dynamic actuator settings. Finally, the azimuthal stiffness is converted to fixed-system values using multi-blade transformations for input to comprehensive rotorcraft prediction codes.

INTRODUCTION

Accurately predicting the dynamic stall characteristics of a helicopter rotor system is one of the many goals of the rotorcraft industry. For the past 19 years, data from the UH-60A Airloads Flight Test (ref. 1) have been used to develop and validate various dynamic stall models. A key parameter for the modeling of the rotor system is the helicopter control system stiffness. The author of this paper, R. Kufeld, measured the control stiffness of the UH-60A helicopter in 1997 (ref. 2). The measured value compared well to a value estimated by Sikorsky and also showed an azimuthal and loading variation.

In May 2010 NASA / Army completed a wind tunnel test of the UH-60A Airloads rotor in the 40- by 80-Foot Wind Tunnel shown in figure 1 (ref. 3). The UH-60A Airloads instrumented rotor was mounted on the Large Rotor Test Apparatus (LRTA) and tested over a large range of thrust and RPM test conditions. Data from this test can be used in much the same way as the flight test data to develop and validate new rotor predictive tools. To help with this validation, measurements of the LRTA control system stiffness are desired, as there are several differences between the aircraft and the LRTA.

The control system stiffness of the LRTA was measured at Ames Research Center in the National Full-Scale Aerodynamic Complex (NFAC) 40- by 80-Foot Wind Tunnel low bay, operated by the U.S. Air Force. The measurements were acquired between August 2011 and October 2011, with the LRTA mounted on its storage and transportation stand. This paper describes the differences between the UH-60A aircraft and the LRTA control systems, discusses

the technique used to measure the control system stiffness, and presents the results of the measurements.

DIFFERENCES BETWEEN AIRCRAFT AND LRTA CONTROL SYSTEMS

A description of the UH-60A aircraft swashplate and stationary links from reference 1 is repeated here to familiarize the reader with the mechanical aspects of the aircraft. Figure 2 shows a schematic of the location of the three UH-60A stationary swashplate links with respect to the rotor azimuth. These stationary links support and supply input to the swashplate and pitch change links and affect the control system stiffness. The three stationary links are located unevenly around the azimuth, 90 degrees apart azimuthally. This leaves half of the swashplate unsupported by a stationary link between the rotor azimuth at 304 degrees and 124 degrees. The UH-60A main rotor has a leading edge pitch link that, when aligned with the forward stationary link, positions one blade spindle nominally to the 90-degree rotor azimuth position. With the stationary links 90 degrees apart, the pitch links for the next two blades are also aligned with stationary links at the 180- and 270-degree azimuth positions.

Figure 3 shows a cutaway view of the UH-60A aircraft control system between the primary servos and the swashplate with the three stationary links clearly labeled. Note that the linkage configuration for the forward and lateral stationary links is essentially the same (primary servo connected to a bell crank then connected to the stationary link). The aft stationary link configuration has an extra bell crank and long control rod within its series to enable the control input to reach the far side of the swashplate where the aft stationary link attaches. These extra components in the aft stationary link series add flexibility to this portion of the control system.



Figure 1. UH-60A Airloads rotor mounted on the LRTA inside the NFAC 40- by 80-Foot Wind Tunnel.

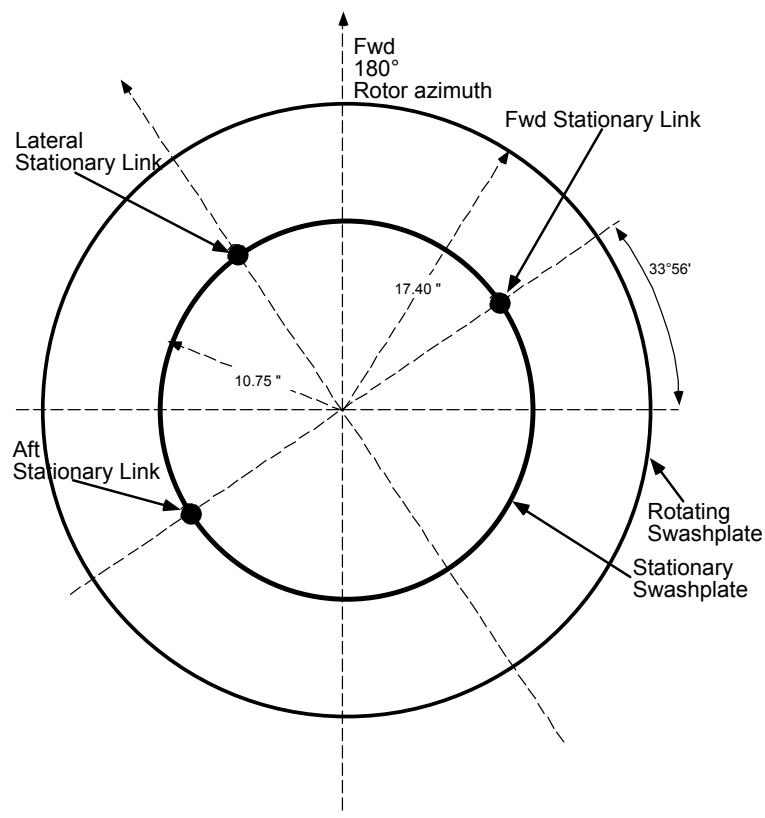


Figure 2. Schematic of the UH-60A and LRTA swashplate and stationary link locations.

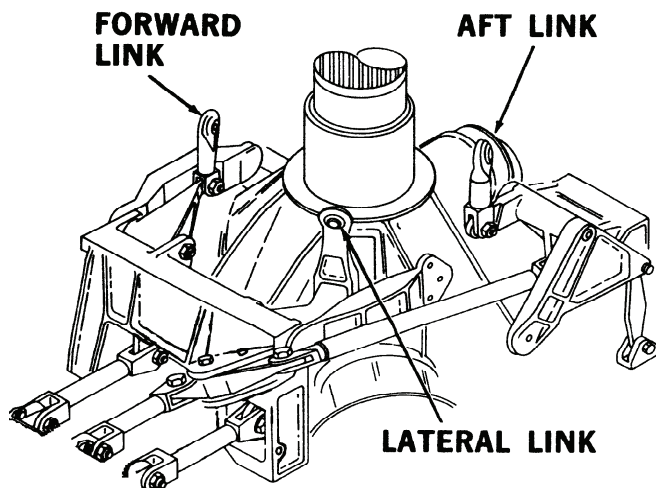


Figure 3. Cutaway view of UH-60A control system linkages.

A brief summary of the LRTA rotor control system is provided here. Reference 4 provides more detail. For the test of the UH-60A rotor on the LRTA (refs. 3-4), flight hardware was used down to and including the swashplate assembly. The forward, lateral, and aft stationary links of the aircraft and every component below the swashplate, however, were replaced with the LRTA control system hardware. The LRTA has three identical rocker arm systems with one end attached to a primary low-speed high-authority actuator and the other end attached to a link that connects to the UH-60A swashplate. Each primary actuator and rocker arm is mounted on the LRTA chassis. The primary actuators are a ball-screw type driven by a servo motor. Also attached to the LRTA rocker arm is a hydraulic rotary reciprocal-type actuator, which is the main component of the dynamic actuator system. Figures 4 and 5 (ref. 5) show schematics of the rocker arm and dynamic actuator systems, and figure 6 is a photograph of a rocker arm and dynamic actuator installed on the LRTA. The dynamic actuator system includes a centered/lock-out mechanism that is activated when the dynamic actuators are turned off to minimize uncontrolled inputs to the swashplate. The lock-out mechanism can also be engaged while the dynamic actuators are active; this limits but does not eliminate actuator motion. The forward and aft links from the rocker arm to the swashplate are identical to each other. However, the lateral link between the rocker and swashplate consists of two different components designed to counteract the rotational loads of the swashplate. Figures 7 and 8 show each of the two different link types. The LRTA primary and dynamic actuator systems each have their own control console, the Primary Control Console (PCC) and Dynamic Control Console (DCC), respectively. Both actuator systems (and control consoles) were used during the UH-60A Airloads wind tunnel test in various combinations. The control stiffness testing therefore required measurements in multiple configurations to fully document the stiffness properties of the system. Details of these configurations are provided later in this report.

The LRTA control stiffness was expected to vary depending on the configuration of the dynamic actuators, “off” or “active”. When they were off, it was expected that the rocker arm/primary actuator assembly would be quite stiff, possibly much stiffer than on the aircraft. When the dynamic actuators were active, it was expected that the control stiffness would be significantly reduced as a result of the working hydraulic system.

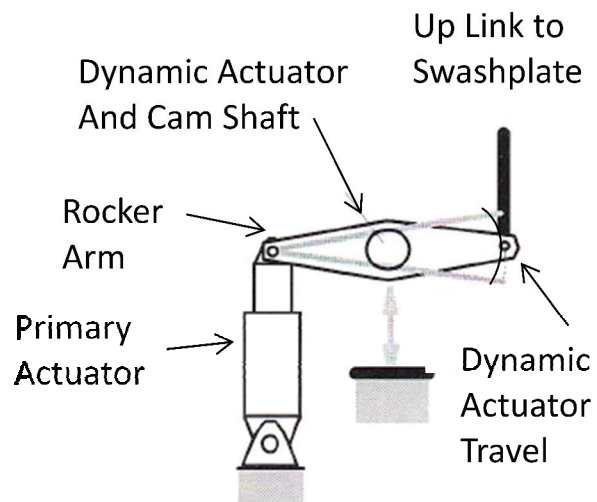


Figure 4. Primary actuator and rocker arm schematic.

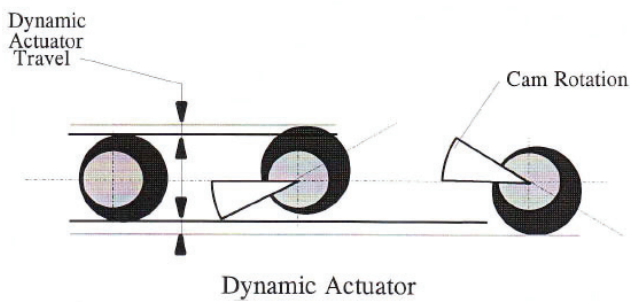


Figure 5. Dynamic actuator schematic.

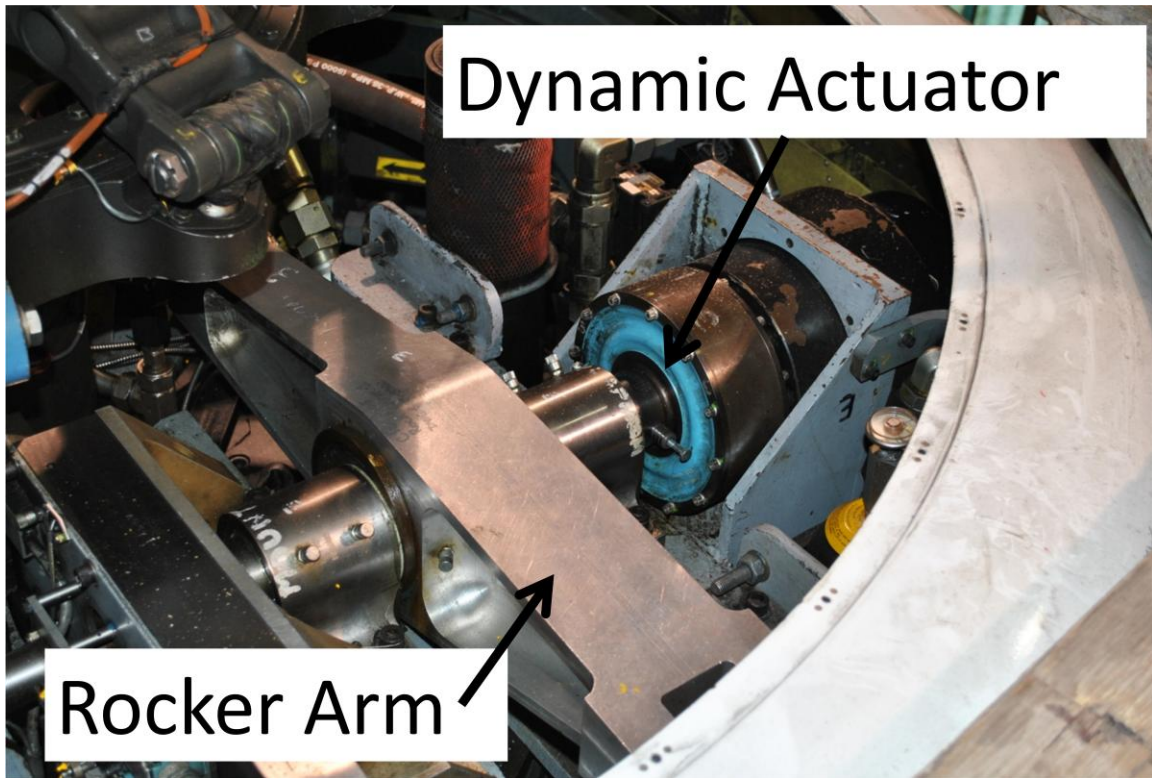


Figure 6. Photograph of LRTA rocker arm and dynamic actuator.

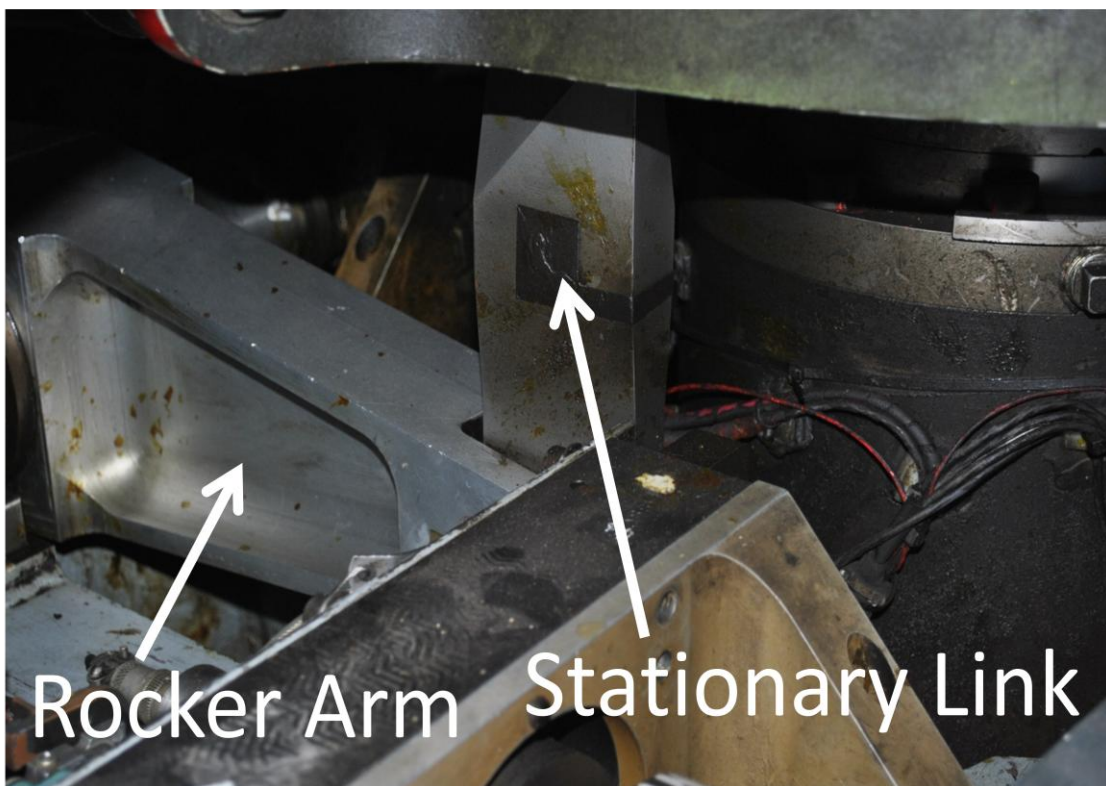


Figure 7. Single stationary link for the forward and aft swashplate connection.

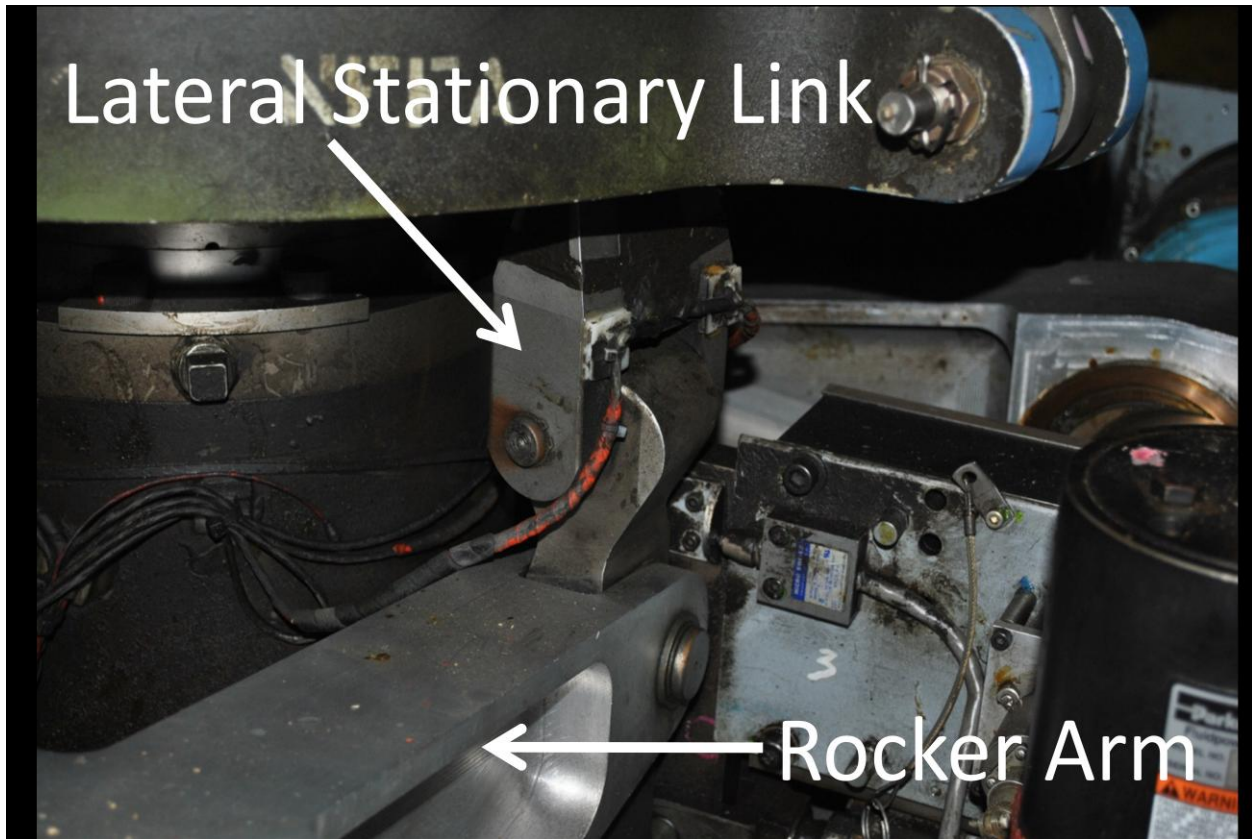


Figure 8. Two-component stationary link for the lateral swashplate connection.

CONTROL SYSTEM STIFFNESS MEASUREMENT TECHNIQUE

The control system measurement objective was to enable the simultaneous measurement of the pitch rotation of all four blade spindles caused by a pure pitch moment input while the controls were commanded to keep a fixed control setting. The pitch motion divided by the applied load is an estimate of the control system stiffness. The test hardware fixed the blade spindles in flap and lag, while only allowing the blades to move in the pitch direction. The hardware also allowed easy and independent load variations for each blade spindle, and had four accurate and independent rotary encoders to measure each spindle rotation. The rotor hub and test hardware were positioned at different azimuthal positions from 0 to 90 degrees, with a step size of 15 degrees, to measure the effect of azimuth position on control system stiffness. A detailed description of the measurement technique, including both the hardware and instrumentation setup and test procedures, is provided in the following sections.

Setup

The LRTA control stiffness was measured inside the NFAC low bay with the UH-60A blades removed. A work platform was installed above the LRTA to allow manual loading and unloading of calibrated weights used to apply a leading-edge-down pitching moment along the feathering axis of the blade. The control stiffness measurement test hardware was similar to the hardware used in the previous UH-60A aircraft control stiffness measurements (ref. 2). Figure 9 shows a schematic of the hardware used during this test. The schematic shows four I-beam supports attached to the UH-60A bifilar ring and four loading moment arms attached to the spindles using adapter blocks. Weight pans (not shown) were attached to the moment arms and manually loaded with calibrated weights to apply a known moment to each blade spindle. The spindle adapter blocks were installed on each of the four spindles using the blade attachment pins, and transferred the pitching moment to the quarter chord feathering axis of the blade spindles and down the pitch change links into the swatchplate and fixed control system.

The adapter blocks served two other functions. The rotation of the spindles was measured with a 16-bit rotary encoder with a resolution of 0.0055 degrees via a load-bearing interface link attached to the adapter blocks. The interface link, positioned at the feathering axis of the blade, had one end fixed to the adapter block and the other end attached to the rotary encoder via a coupling flexible in bending only. The adapter block and interface link assembly were also used to position the spindle flap and lag position to a nominal condition similar to a wind tunnel test condition. To lock the spindles in place, the interface link was passed through a rod end attached to the I-beam supports. This configuration not only fixed the flap and lag position of each spindle while allowing a full range of pitch motion, but also absorbed most of the vertical shear load of the dead weight and passed it along to the transmission. The average flap angle measured for the four blades was 4.6 degrees while the unmeasured lag angle was approximately 7 degrees. Figure 10 shows a close-up view of the test setup near one of the UH-60A hub spindles. The test hardware on the other three spindles was installed in the same manner. Figure 11 shows a close-up view of the interface link attached to the adapter block passing through the rod end and connecting to the rotary position encoder via a flexible coupling.

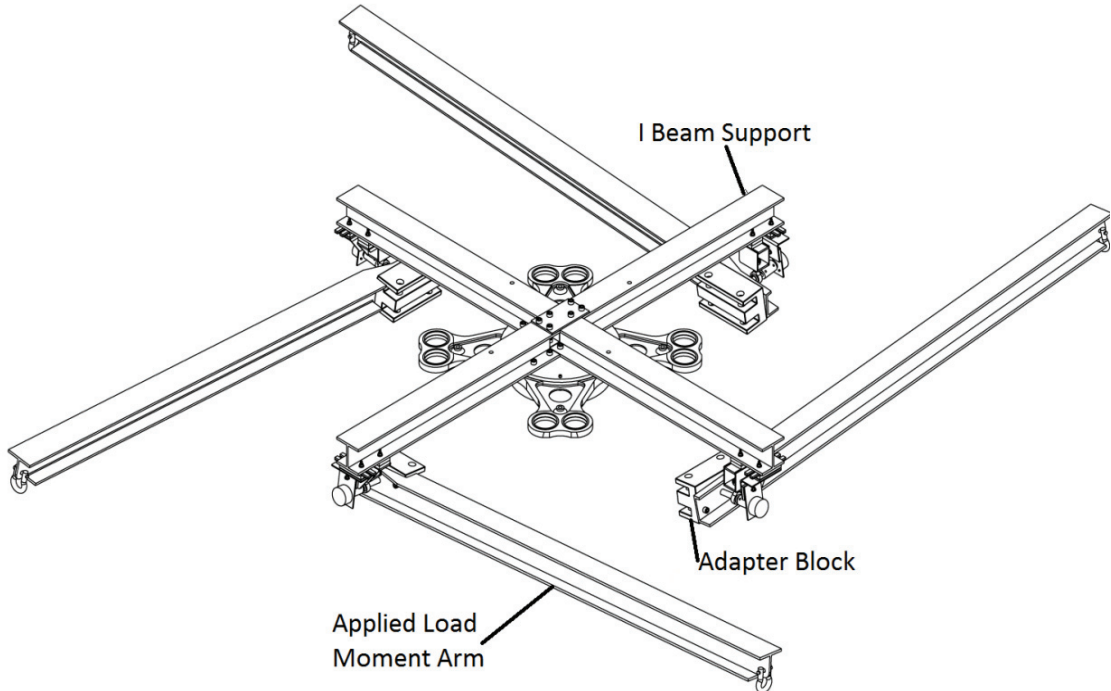


Figure 9. Schematic of control stiffness measurement hardware.

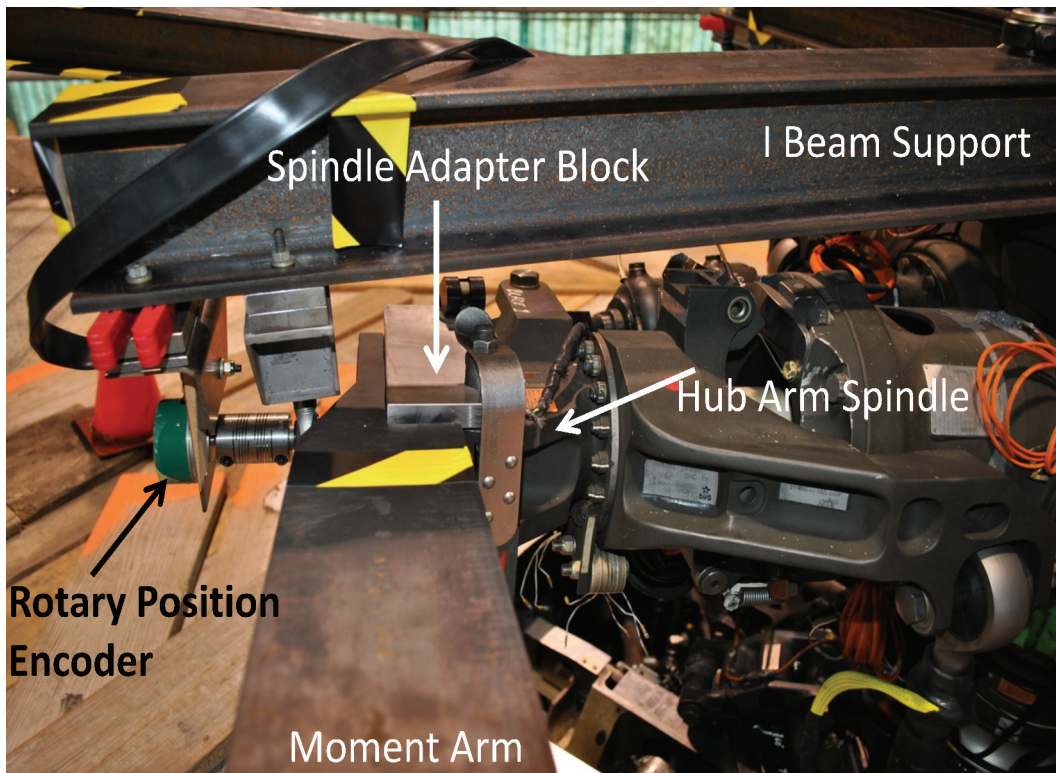


Figure 10. Photo of UH-60A hub spindle with control stiffness measurement hardware installed.

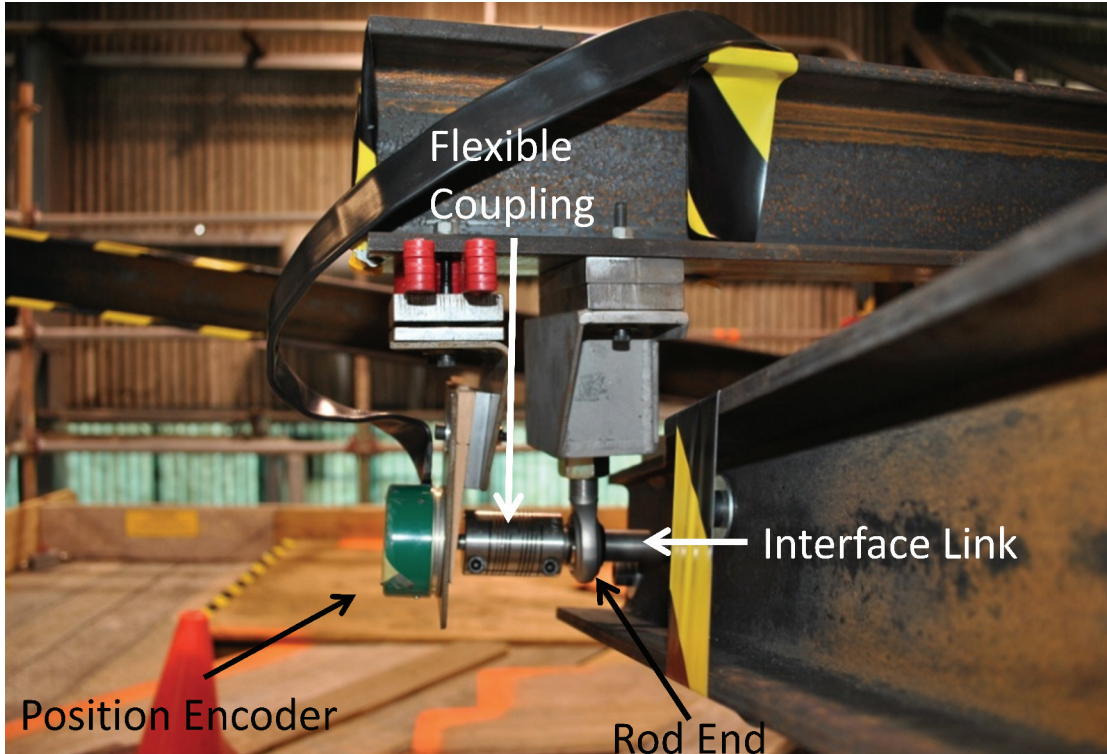


Figure 11. Detailed photo of the interface link passing through a rod end and connecting to the position encoder via a flexible coupling.

Testing Procedure

To prepare for the day's testing, the PCC was turned on. Hydraulic pressure was supplied by a portable hydraulic cart. A collective loading pre-load run was performed to exercise the hysteresis of the control system bearings. The PCC was active for all testing, and the controls were set to a nominal flight condition of 9 degrees of collective and 0 degrees of both longitudinal and lateral cyclic pitch. The DCC was off with the dynamic actuators in the locked-out condition for non-dynamic actuator active control stiffness measurements. The DCC was active, with the dynamic actuators in the locked-out condition, supplying a high-frequency random drive signal with an average displacement of zero to all dynamic actuators for dynamic actuator active control stiffness measurements. This DCC configuration was selected because it was determined during preliminary testing that the dynamic actuator had a large dither motion resulting in a dangerous situation for the manual loading of the calibrated weights. To increase safety and provide consistent results, the dither was reduced and the dynamic actuators were locked out during testing. Measurements were made to ensure that active dynamic actuators in the locked-out condition still had enough free movement to provide an accurate measurement of the control stiffness. Figure 12 compares the time history of the encoder measurements for the two different types of dynamic actuator testing conditions mentioned above. Testing with one or both of the control systems active was required to match test conditions from the wind tunnel test.

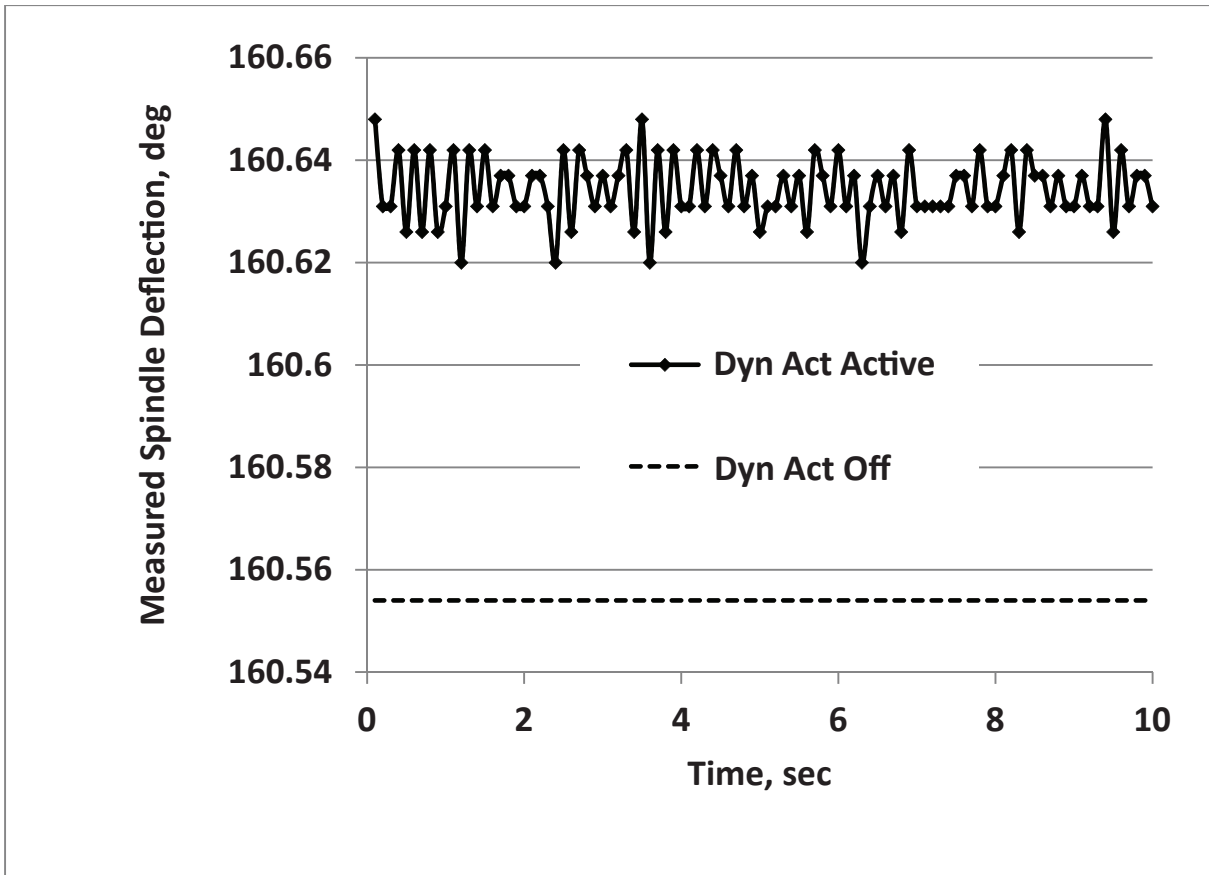


Figure 12. Time history measurement of blade 2 with dynamic actuators active and off:
270-degree azimuth, collective loading.

The four blade spindles were manually loaded simultaneously with a nose-down pitching moment by applying calibrated weights to the moment arms in one of three loading techniques (collective, cyclic, reactionless) described on the following page. These loading techniques estimated the three different modes of the control system model in some comprehensive analysis. The collective loading models the loading of all four blades reacted by the fixed-system control system. Cyclic loading models the loading of two opposite blades reacted by the fixed-system control system. The reactionless loading models the loading of only one blade reacted by the fixed-system control system. With the loading and spindle deflection stable, a measurement was recorded and loading for the next data point began. A series of 21 data points were used for one test condition to determine the level of linearity and to allow for curve fitting of nonlinear results. The estimates of control stiffness were calculated from the delta pitch deflections and delta applied pitching moments from the starting spindle pitch positions and pitching moments.

The hub position was determined by aligning the blade pitch links with the swashplate stationary links, and blade 1 was near the wind tunnel test zero azimuth position so this was called the zero azimuth position. When a loading cycle was completed with the hub in this position, the hub was rotated in 15-degree increments, measured with a transit mounted on top of the hub at the center of rotation, and addition loadings were performed.

Measurements were made on all four blades simultaneously. The nominal load sequence started with a preload of 50 pounds and moved up to 250 pounds in 20-pound increments and then back down to 50 pounds for a total of 21 measurements. This resulted in an applied maximum nose-down pitch moment delta on the control system of 1186 foot-pounds per blade. As mentioned previously, different loading conditions were tested:

1. Collective loading: all four blades spindles were loaded simultaneously in the same direction from 50 to 250 pounds.
2. Reactionless loading: all blade spindles started with a 150-pound load; two opposite spindles (e.g., blades at 0 degrees and 180 degrees) increased their loading to 250 pounds while the other set of opposite spindles (e.g., 90 degrees and 270 degrees) decreased their loading to 50 pounds. Once the maximum load condition was reached, the loading was reversed. When the loading reached the other extreme loading condition the loading was reversed again, and the test was completed when all spindles were back at the starting point of 150 pounds.
3. Cyclic loading: again starting with 150 pounds on all four blades spindles, the loading only changed on one set of opposite blades (e.g., 0 degrees and 180 degrees). Loading on one blade increased to 250 pounds while the loading on the opposite blade decreased to 50 pounds. The load on the 90- and 270-degree blade spindle remained constant. For faster testing, the hub was not rotated and the cyclic loading was on the blade spindles in the 90- and 270-degree azimuth position.

Once a loading cycle was completed, the hub was rotated 15 degrees to a new azimuth position and the loading cycle was repeated. The loading was performed at seven different azimuth positions in all to cover the full rotation of the rotor. The first and last azimuth position measurements provided one set of repeated data points of a different blade spindle at the same azimuth position (0, 90, 180, and 270 degrees). The average collective pitch angle was measured at 9.75 degrees, the average flap angle was measured at 4.5 degrees, and the lead-lag angle was not measured. Figure 13 shows a maximum collective loading condition with 250 pounds on all four spindles hanging from the 6-foot moment arms.

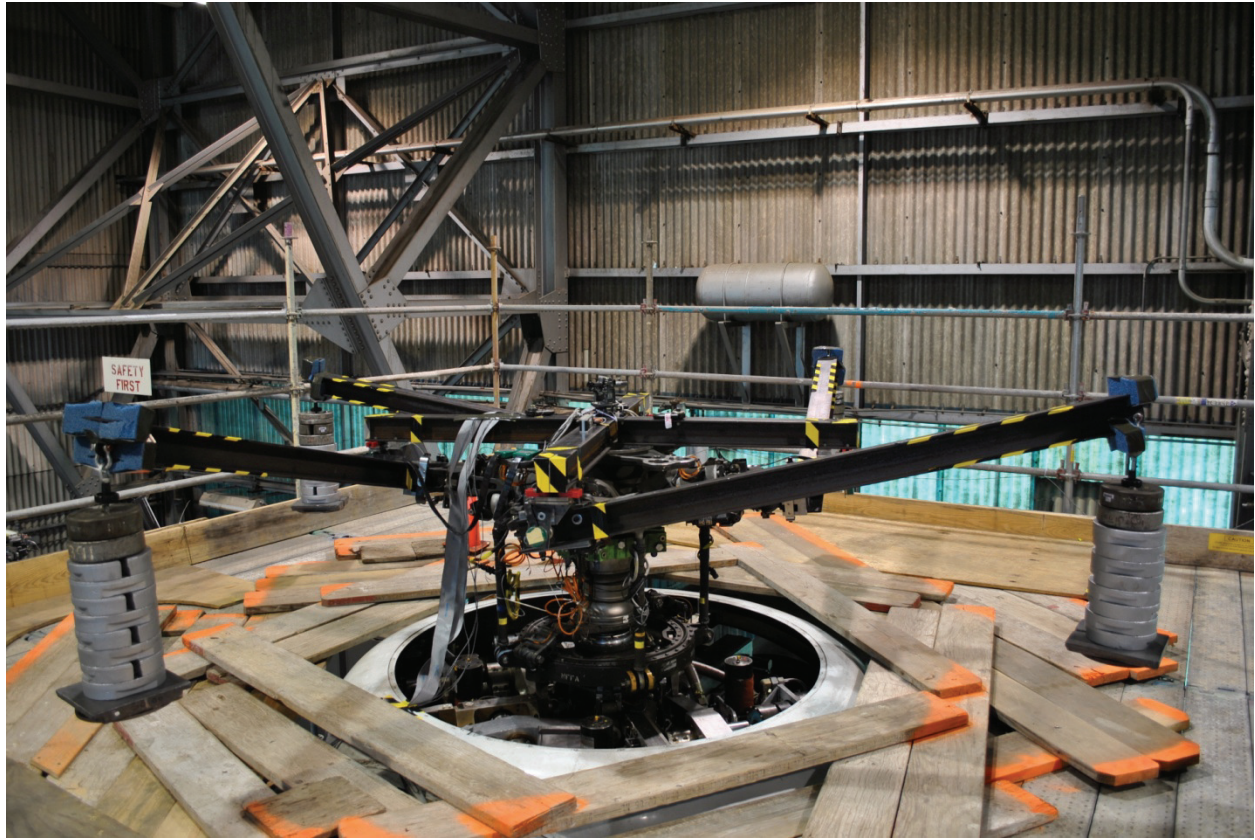


Figure 13. Maximum collective loading condition, 250 pounds hanging from all four moment arms.

RESULTS

The measured spindle pitch deflection and applied moment for all blades under the three different loading conditions with the dynamic actuator active and off are shown in tables 2–7 in the appendix of this paper. The slopes of the resultant curves were calculated with a least-square curve fit, and these values were the estimate of the control system stiffness at the given azimuth. The control stiffness estimates for collective, reactionless, and cyclic loading compared to aircraft measurements are shown in tables 8–10 in the appendix of this paper. Unfortunately the determination of the slope often required some engineering judgment, as the blade spindle would deflect in a nonlinear manner near the 180-degree azimuth position. The data could be loosely fitted into one of four different categories that were mostly based on azimuth position of the blade spindle during testing. Figure 14 shows typical results from a blade spindle near the 90- or 270-degree position. This shows very little hysteresis from the two different loading directions. When the pitch links were near the stationary swashplate links (near 90 degrees and 270 degrees) this very stiff structure was the major contributor to the stiffness. As the spindles move away from the stationary links towards 0-degree azimuth position the effect of the unsupported swashplate is seen in the data as a larger hysteresis loop. Figure 15 shows a small to medium hysteresis loop and a relatively large angle deflection of the blade spindle.

As the spindle azimuth position moves away from the 90-degree azimuth position towards the 180-degree position the measurements show a nonlinear behavior. Figure 16 is a typical plot of data measured near the 180-degree azimuth position. Although the exact reason for this behavior is not known, there are some mechanical differences in this location that can contribute to the nonlinear behavior. First, the extra stationary link between the swashplate and the rocker arm may move a small amount due to bolt clearance. There also is the lack of an opposing stationary link in the 0-degree position to provide the extra stability found near the 90- and 270-degree position. As this position on the swashplate is the stiffest (smallest pitch deflection) nonlinear motion is magnified by small overall pitch deflection.

The fourth category of stiffness measurement behavior was found during cyclic loading near the 180-degree azimuth position. Here the stiffness shows a dead band as the loading transitions from one side of the swashplate to the other. Figure 17 shows an example of this measurement. To estimate the stiffness from this type of data the dead band data was ignored, and an average of the slopes of the upper half and the lower half of the loading was used for the estimate of stiffness.

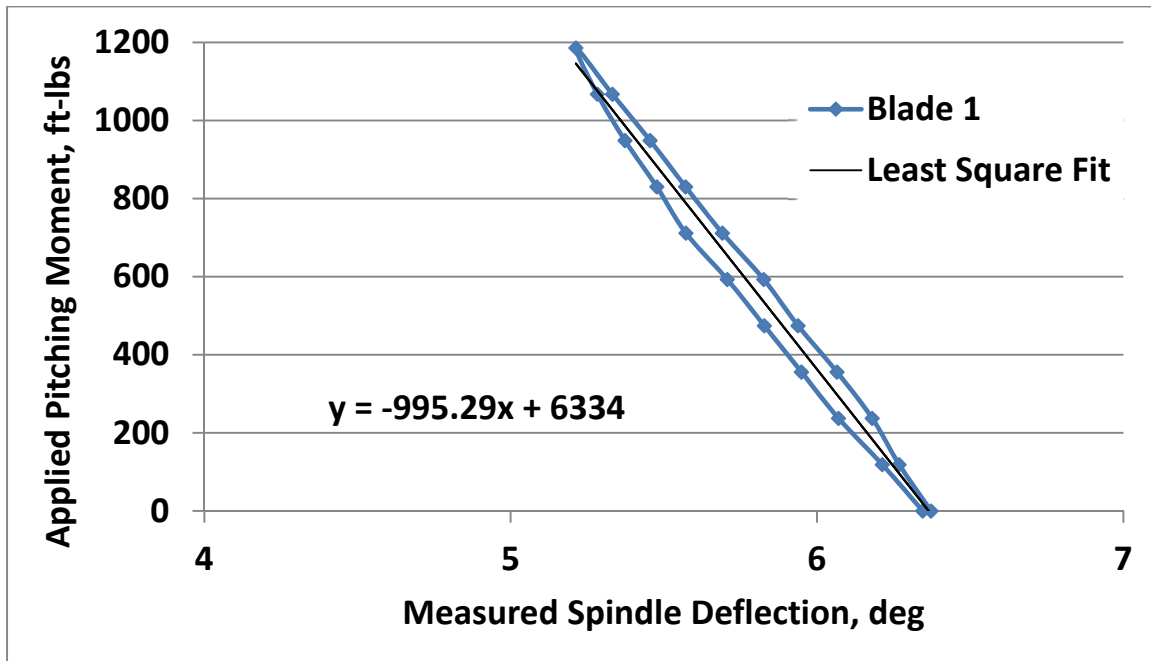


Figure 14. Typical measurement results for blade spindle near the 90- or 270-degree azimuth position: blade 1, collective loading, 75-degree rotor azimuth, and dynamic actuators off, linear equation shown.

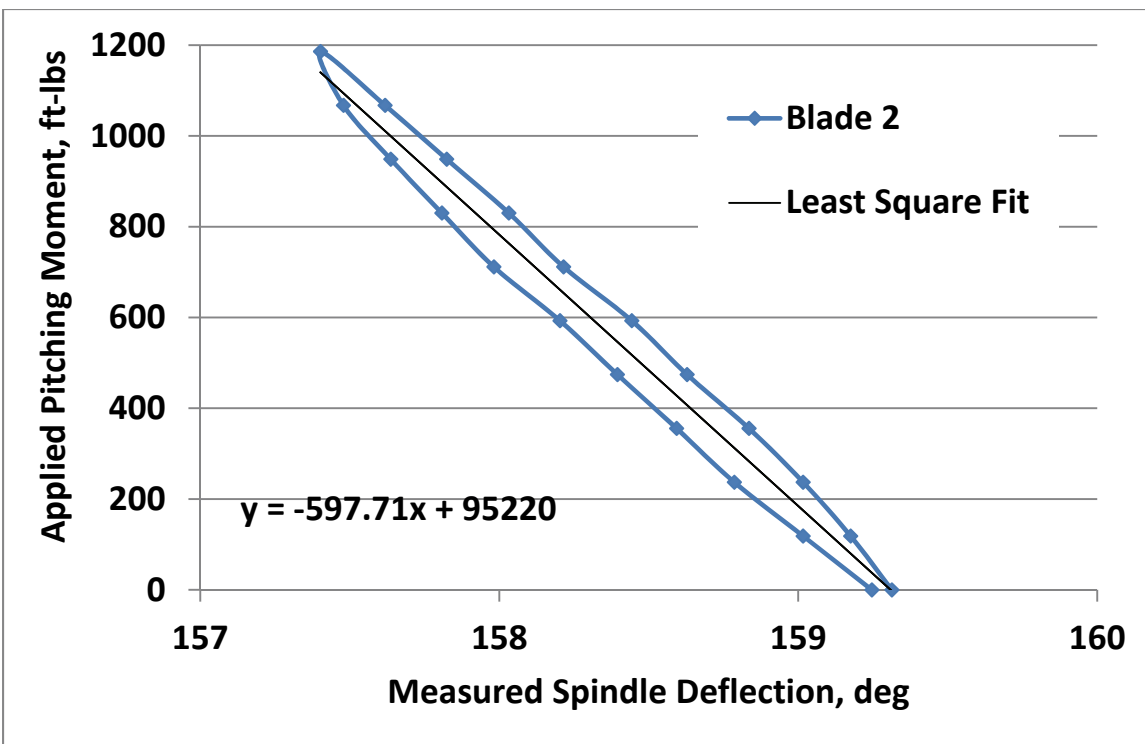


Figure 15. Typical measurement results for blade spindle near the 0-degree azimuth position: blade 2, collective loading, 345-degree rotor azimuth, and dynamic actuators off, linear equation shown.

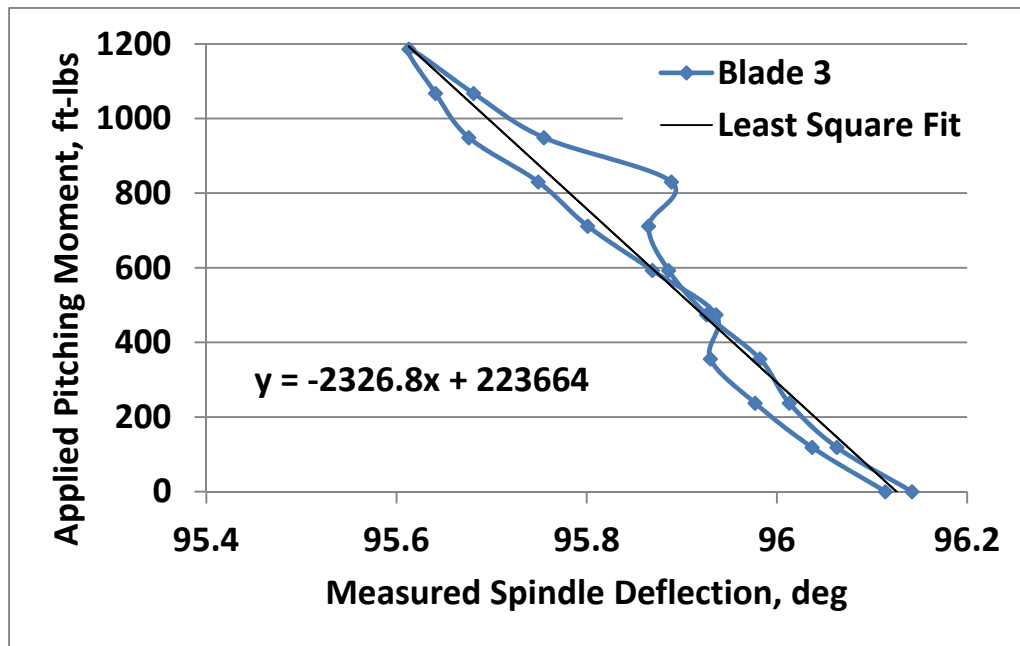


Figure 16. Typical measurement results for blade spindle near the 180-degree azimuth position: blade 3, collective loading, 195-degree rotor azimuth, dynamic actuators active, and linear equation shown.

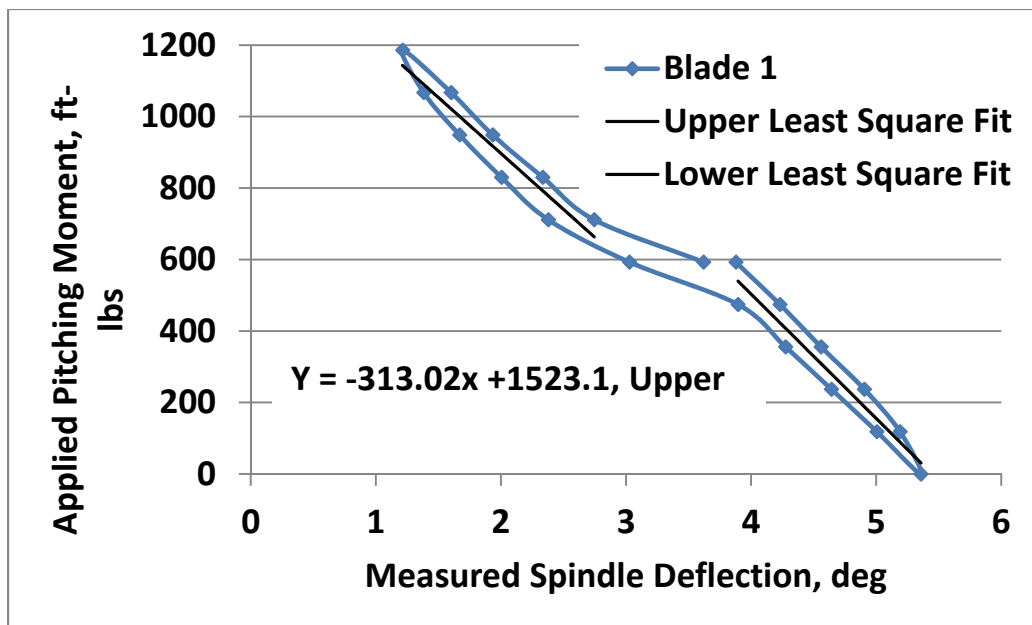


Figure 17. Typical measurement results for blade spindle under cyclic loading: blade 1, cyclic loading, 15-degree rotor azimuth, dynamic actuator off, linear equations for upper half of data and lower half of data.

The slopes (units of control stiffness, foot-pounds/degree) for all azimuth position loading conditions and dynamic actuator states (active and off) were calculated and compared to the aircraft stiffness measured in 1997 as a function of rotor azimuth. Figures 18–20 show the comparison of the three different loading conditions: collective, reactionless, and cyclic. For each of the three loading conditions there was not a significant difference between dynamic actuators active/locked-out and off. This was unexpected and resulted in further research into the mechanics of the dynamic actuator system. It was discovered that the dynamic actuators are always supported by hydraulic fluid for both active and off operating conditions, resulting in the same stiffness for both operating conditions. For all three loading conditions the results were similar to the measurement made on the aircraft in 1997. For the collective loading (fig. 18), the LRTA control stiffness was slightly higher than the aircraft. Near the stiffest part of the swashplate, 180 degrees, the LRTA stiffness was measured near 2500 foot-pounds/degree compared to 2200 foot-pounds/degree for the aircraft. It was also apparent on the retreating part of the azimuth (between 180 and 360 degrees) that the LRTA was stiffer than the aircraft. This was attributed to the mechanical differences of the two control systems. The retreating side portion of the aircraft was supported by the aft stationary link, which was connected to the servo by a long, relatively flexible control rod. The very stiff aft rocker arm assembly supports the retreating side of the LRTA. The higher stiffness around the rest of the azimuth was also attributed to the stiffer rocker arms/stationary links supporting the swashplate.

For the reactionless loading (fig. 19), all three measurements of control stiffness were nearly identical. This was expected as this loading was designed to reduce the effect of the stationary link loads and was a measure of the stiffness of the swashplate and pitch links only. The effects of the stiffer LRTA control system still can be seen near the 180- and 270-degree position. The measured control stiffness for cyclic loading shows the most difference compared to the aircraft. As mentioned previously, the stiffness on the retreating side of the aircraft is less due to the long, relatively flexible control rod connecting the stationary link to the primary servo. This effect is more pronounced with cyclic loading. The LRTA cyclic loading control stiffness is symmetrical about the 0- to 180-degree axis and greater than the aircraft. The identical, stiffer rocker arm stationary links contribute to the 900 foot-pounds/degree stiffness at the 90- and 270-degree azimuthal positions. The LRTA stiffness matches the aircraft near the 0- and 180-degree azimuthal positions as the unsupported end of the swashplate near 0-degree azimuth dominates this measurement, which is the same for both the aircraft and the LRTA.

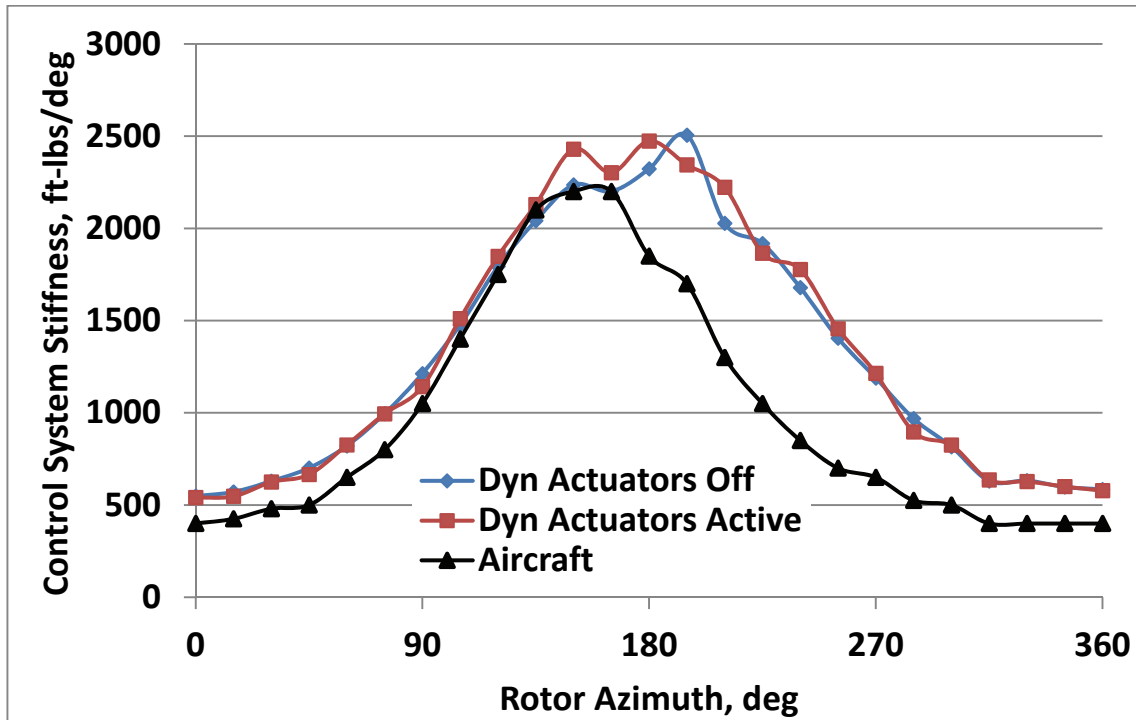


Figure 18. Azimuthal variation of LRTA control stiffness for collective loading with the dynamic actuators active and off compared to UH-60A aircraft.

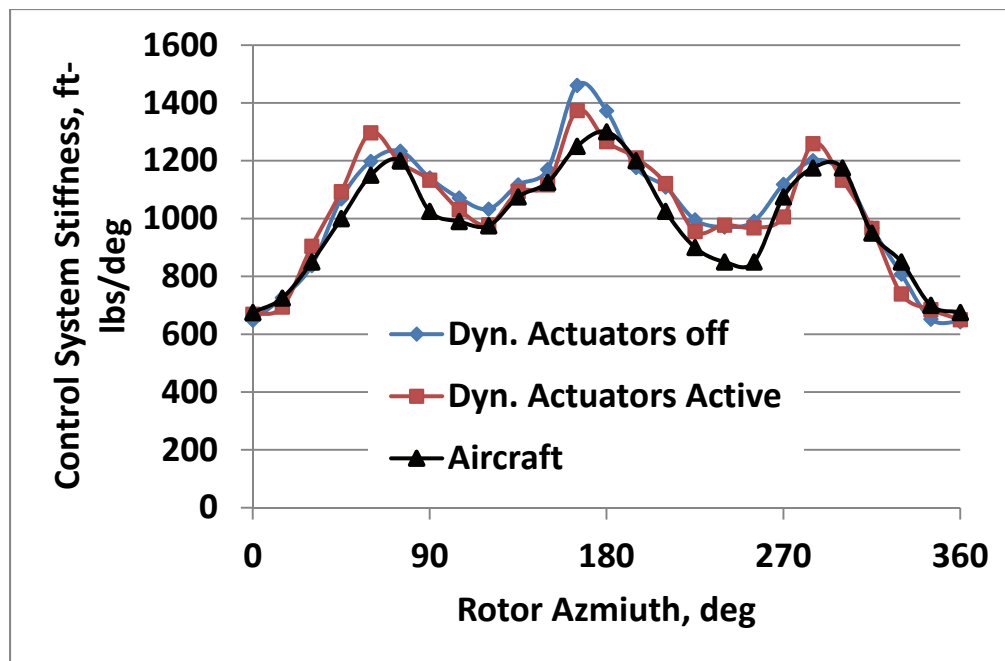


Figure 19. Azimuthal variation of LRTA control stiffness for reactionless loading with the dynamic actuators active and off compared to UH-60A aircraft.

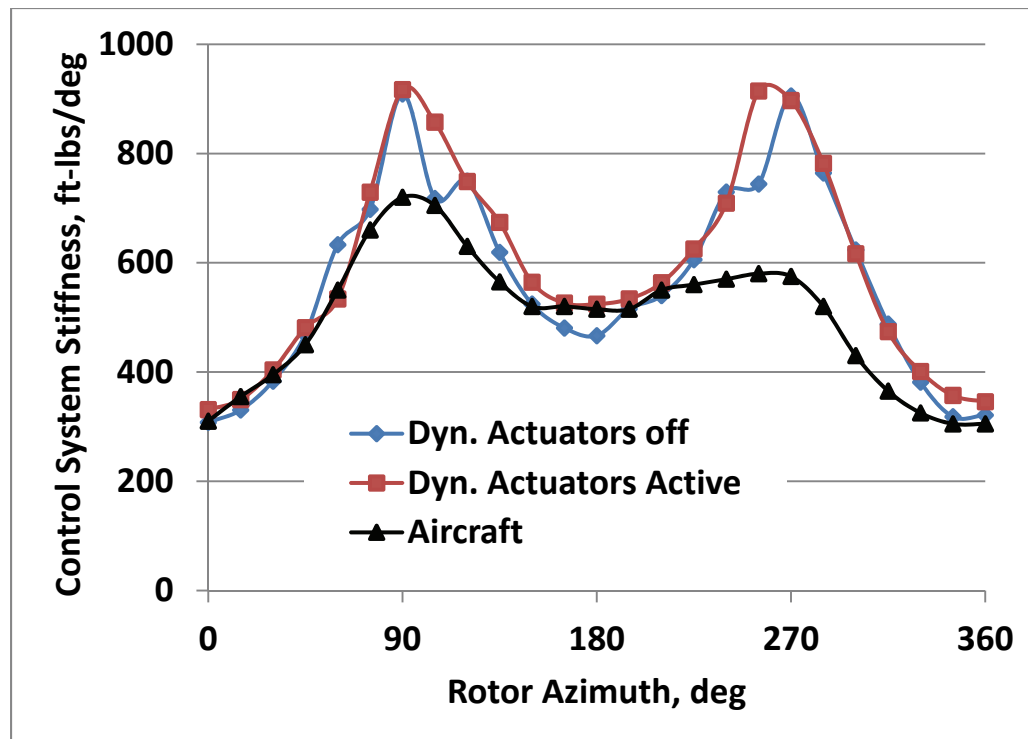


Figure 20. Azimuthal variation of LRTA control stiffness for cyclic loading with the dynamic actuators active and off compared to UH-60A aircraft.

MULTI-BLADE COORDINATE TRANSFORMATIONS

The azimuthal measured stiffness can be converted to fixed-system stiffness using multi-blade coordinate transformations (ref. 6) to estimate the values for input to comprehensive rotorcraft prediction codes such as CAMRAD II. The measured data from the three loadings are used with the four equations (eqs. 1–4) to calculate fixed-system stiffness. The cyclic loading data is split into two different components (sine and cosine) to supply the proper input for the equations. For accurate calculations using these equations, the proper sign of the stiffness needs to be carefully book kept. The stiffness for loadings using opposite directions (reactionless and cyclic loadings) has opposite signs. In addition, the fixed-system stiffness for cyclic loading requires a rotation transformation back to the longitudinal and lateral axes of the aircraft. If done correctly, the sine and cosine fixed-system cyclic values will be nearly constant around the azimuth. As such, average values of the stiffness have been calculated from the seven different azimuth positions measured for each loading configuration. The results of the calculations are presented in equation 5 for dynamic actuators off and equation 6 for dynamic actuators active, and can be compared to the results for the aircraft in equation 7 (ref. 2). The diagonal of the 4 x 4 fixed-system stiffness matrices would be the required inputs for a comprehensive rotorcraft prediction code.

Figures 21 and 22 show the transformed values of the primary stiffness (e.g., collective stiffness during collective testing) for each of the six different azimuthal loadings with the dynamic actuator off and dynamic actuator active.

$$K_{\text{col}} = \frac{1}{N} \sum_{m=1}^N K_{(m)} \quad \text{Eq. (1)}$$

$$K_{\cos} = \frac{2}{N} \sum_{m=1}^N K_{(m)} \cos \psi_m \quad \text{Eq. (2)}$$

$$K_{\sin} = \frac{2}{N} \sum_{m=1}^N K_{(m)} \sin \psi_m \quad \text{Eq. (3)}$$

$$K_{\text{react}} = \frac{1}{N} \sum_{m=1}^N K_{(m)} (-1)^m \quad \text{Eq. (4)}$$

Where $K_{(m)}$ is measured stiffness for the m th blade, ψ_m is azimuth position of the m th blade, and N is the number of blades.

$$\begin{Bmatrix} M_{\text{col}} \\ M_{\cos} \\ M_{\sin} \\ M_{\text{react}} \end{Bmatrix} = \begin{bmatrix} 1329 & -896 & 29 & -6 \\ -44 & 418 & -1 & 9 \\ -3 & 91 & 699 & 22 \\ 24 & 5 & 4 & 1051 \end{bmatrix} \begin{Bmatrix} \theta_{\text{col}} \\ \theta_{\cos} \\ \theta_{\sin} \\ \theta_{\text{react}} \end{Bmatrix} \quad \begin{array}{l} \text{Dynamic actuators off} \\ \text{Eq. (5)} \end{array}$$

$$\begin{Bmatrix} M_{col} \\ M_{cos} \\ M_{sin} \\ M_{react} \end{Bmatrix} = \begin{bmatrix} 1354 & -952 & 35 & -7 \\ -53 & 496 & -6 & 9 \\ -4 & -6 & 713 & 43 \\ 7 & 2 & -10 & 1036 \end{bmatrix} \begin{Bmatrix} \theta_{col} \\ \theta_{cos} \\ \theta_{sin} \\ \theta_{react} \end{Bmatrix}$$

Dynamic actuators
active
Eq. (6)

$$\begin{Bmatrix} M_{col} \\ M_{cos} \\ M_{sin} \\ M_{react} \end{Bmatrix} = \begin{bmatrix} 897 & -135 & 57 & -32 \\ -357 & 534 & -13 & -14 \\ -28 & 1 & 698 & -53 \\ -53 & 18 & 15 & 1090 \end{bmatrix} \begin{Bmatrix} \theta_{col} \\ \theta_{cos} \\ \theta_{sin} \\ \theta_{react} \end{Bmatrix}$$

Aircraft
Eq. (7)

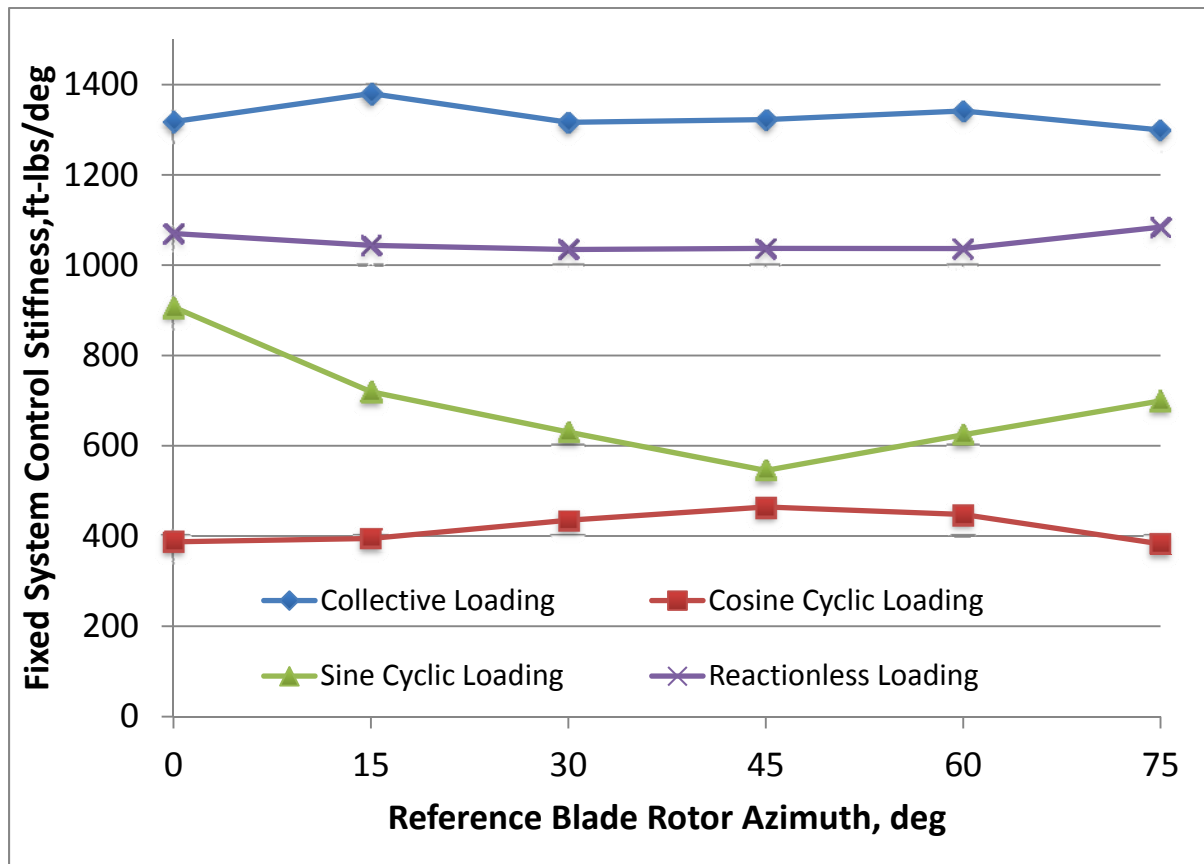


Figure 21. Diagonal elements of the fixed-system control stiffness as a function of the reference blade azimuth position for dynamic actuators off.

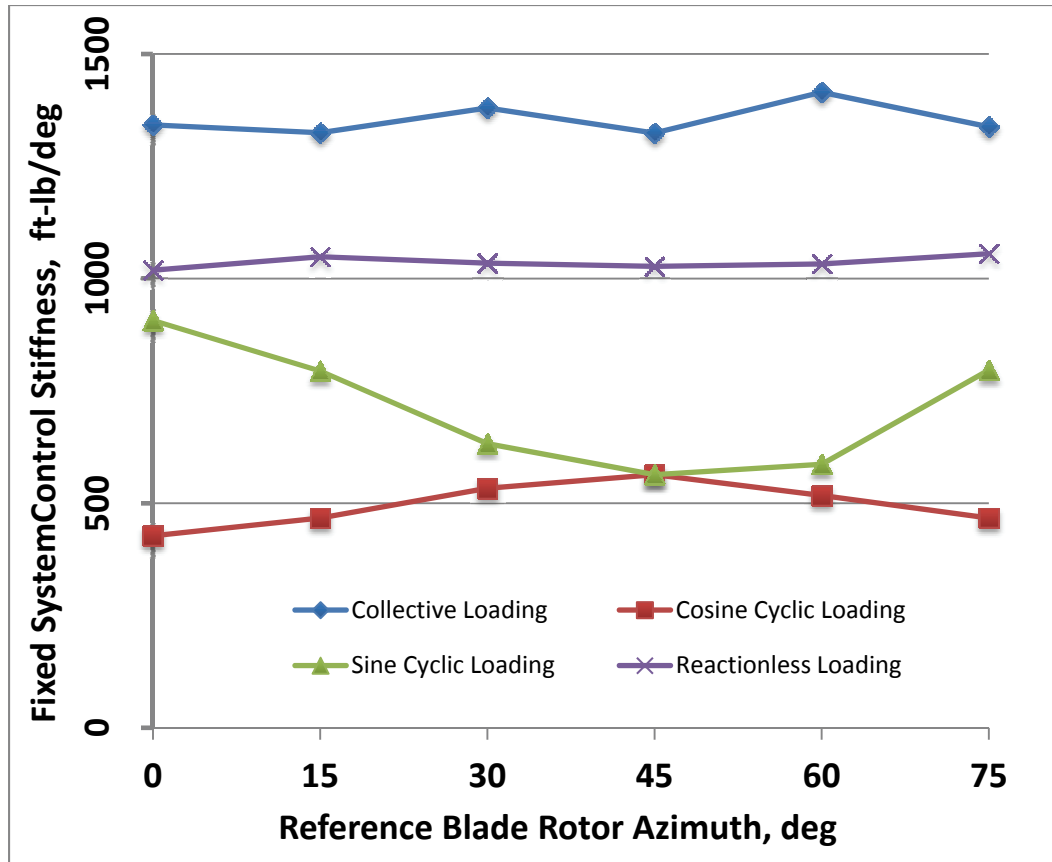


Figure 22. Diagonal elements of the fixed-system control stiffness as a function of the reference blade azimuth position for dynamic actuators active.

CONCLUSION

The control system stiffness of the LRTA with UH-60A rotor hub installed was measured using a technique similar to control system stiffness measurements of the UH-60A Airloads Aircraft performed in 1997. Details of the LRTA control system were presented and compared to the aircraft. Schematics of the test setup and test procedures were also discussed. Three different loading types were used: collective, reactionless, and cyclic. The measurements were made with the dynamic actuators of the control system both active/locked-out and off to match wind tunnel testing conditions. The results show the measured stiffness for the dynamic actuators active/locked-out and off are nearly identical for all loading types. These results were unexpected but are believed correct after a study of the dynamic actuators locked-out configuration. The LRTA azimuthal collective stiffness compares well with the aircraft, with a slightly higher stiffness (as expected) due to the stiffer fixed-system portion of the LRTA control system. The LRTA azimuthal reactionless stiffness is nearly identical to the aircraft because this loading type reduces the effects of the fixed-system portion of the control system (the main difference between the aircraft and the LRTA). The azimuthal cyclic stiffness showed the biggest difference between the LRTA and the aircraft. These differences can be explained by comparing the

difference in the fixed portion of the LRTA and aircraft control system. Finally, the measured azimuthal stiffness was converted to a fixed-system stiffness using multi-blade coordinate transformations to estimate the values for input of the fixed-system stiffness required for comprehensive rotorcraft prediction codes.

REFERENCES

1. Kufeld, R.M.; Balough, D.L.; Cross, J.L.; Studebaker, K.F.; Jennison, C.D.; and Bousman, W.G.: Flight Testing of the UH-60A Airloads Aircraft. 50th Annual American Helicopter Society Forum, Washington, D.C., May 1994.
2. Kufeld, R.M. and Johnson W.: The Effects of Control System Stiffness Models on the Dynamic Stall Behavior of a Helicopter. Journal of the American Helicopter Society, Oct. 2000.
3. Norman, T.R.; Shinoda, P.M.; Peterson, R.L.; and Datta, A.: Full-Scale Wind Tunnel Test of the UH-60A Airloads Rotor. American Helicopter Society 67th Annual Forum, Virginia Beach, VA, May 2011.
4. Norman, T.R.; Shinoda, P.M.; Kitaplioglu, C.; Jacklin, S.A.; and Sheikman, A.: Low-Speed Wind Tunnel Investigation of a Full-Scale UH-60 Rotor System. American Helicopter Society 58 Annual Forum, Montreal, Canada, June, 2002.
5. Henry, M.: Large Rotor Test Apparatus Operation and Maintenance Manual. Dec. 1996.
6. Johnson, W.: Helicopter Theory, Princeton University Press, Princeton, New Jersey, 1980, pp. 350–351.

APPENDIX

TABLE 1. SUMMARY TO IDENTIFY DATA FOR DIFFERENT LOADINGS AND DYNAMIC ACTUATOR CONDITIONS

Loading	Dynamic Actuator Status	Table Number
Collective	Off/Locked Out	2
Reactionless	Off/Locked Out	3
Cyclic	Off/Locked Out	4
Collective	Active/Locked Out/Dither	5
Reactionless	Active/Locked Out/Dither	6
Cyclic	Active/Locked Out/Dither	7

TABLE 2. COLLECTIVE LOADING DYNAMIC ACTUATORS OFF AND LOCKED OUT

	Blade 1 Deflection, deg						
Rotor Azimuth	0°	15°	30°	45°	60°	75°	90°
Applied Load ft-lb							
0.0	4.493	4.669	4.977	5.361	5.889	6.372	6.806
118.6	4.301	4.537	4.828	5.284	5.773	6.268	6.725
237.2	4.109	4.395	4.686	5.142	5.664	6.180	6.633
355.8	3.901	4.125	4.533	4.982	5.521	6.065	6.537
474.4	3.680	3.955	4.340	4.812	5.372	5.938	6.438
593.0	3.450	3.768	4.143	4.647	5.213	5.826	6.345
711.6	3.289	3.554	3.934	4.450	5.080	5.691	6.246
830.2	3.071	3.339	3.757	4.262	4.928	5.571	6.154
948.8	2.771	3.115	3.567	4.114	4.795	5.455	6.051
1067.4	2.577	2.917	3.352	3.944	4.661	5.332	5.955
1186.0	2.329	2.683	3.164	3.775	4.490	5.213	5.851
1067.4	2.453	2.774	3.259	3.845	4.570	5.283	5.922
948.8	2.636	2.911	3.400	3.966	4.669	5.373	6.004
830.2	2.807	3.038	3.527	4.103	4.783	5.477	6.081
711.6	3.009	3.246	3.702	4.267	4.905	5.572	6.180
593.0	3.208	3.448	3.884	4.427	5.059	5.707	6.268
474.4	3.422	3.669	4.081	4.603	5.207	5.828	6.372
355.8	3.642	3.878	4.277	4.789	5.383	5.949	6.471
237.2	3.862	4.114	4.508	4.969	5.531	6.070	6.585
118.6	4.104	4.329	4.697	5.158	5.685	6.213	6.696
0.0	4.312	4.570	4.906	5.345	5.850	6.345	6.795

TABLE 2. CONTINUED

	Blade 2 Deflection, deg						
Rotor Azimuth	270°	285°	300°	315°	330°	345°	360°
Applied Load, ft-lb							
0.0	160.554	160.164	159.807	159.527	159.379	159.313	159.379
118.6	160.477	160.060	159.670	159.417	159.225	159.175	159.274
237.2	160.385	159.965	159.555	159.280	159.060	159.016	159.104
355.8	160.291	159.813	159.434	159.120	158.890	158.835	158.899
474.4	160.192	159.704	159.291	158.950	158.708	158.628	158.681
593.0	160.087	159.577	159.137	158.794	158.500	158.443	158.502
711.6	160.005	159.461	158.978	158.594	158.331	158.215	158.313
830.2	159.906	159.346	158.840	158.391	158.127	158.032	158.116
948.8	159.809	159.216	158.692	158.247	157.951	157.824	157.902
1067.4	159.703	159.082	158.538	158.066	157.783	157.618	157.687
1186.0	159.604	158.961	158.385	157.896	157.555	157.402	157.470
1067.4	159.670	159.027	158.467	157.967	157.654	157.479	157.577
948.8	159.747	159.115	158.577	158.093	157.790	157.637	157.742
830.2	159.835	159.208	158.676	158.220	157.922	157.808	157.928
711.6	159.928	159.329	158.809	158.373	158.087	157.982	158.088
593.0	160.027	159.443	158.953	158.549	158.286	158.203	158.313
474.4	160.131	159.565	159.104	158.719	158.467	158.395	158.478
355.8	160.225	159.691	159.258	158.899	158.725	158.593	158.683
237.2	160.329	159.829	159.428	159.076	158.890	158.786	158.973
118.6	160.422	159.957	159.576	159.274	159.092	159.016	159.197
0.0	160.543	160.098	159.741	159.461	159.318	159.246	159.351

TABLE 2. CONTINUED

	Blade 3 Deflection, deg						
Rotor Azimuth	180°	195°	210°	225°	240°	255°	270°
Applied Load, ft-lb							
0.0	96.114	95.993	95.740	95.389	94.982	94.554	94.131
118.6034	96.075	95.918	95.685	95.276	94.894	94.466	94.026
237.2068	96.029	95.817	95.592	95.210	94.820	94.370	93.933
355.8101	95.982	95.823	95.510	95.142	94.737	94.288	93.824
474.4135	95.949	95.752	95.449	95.083	94.669	94.204	93.713
593.0169	95.905	95.696	95.405	95.015	94.603	94.114	93.610
711.6203	95.839	95.652	95.372	94.971	94.521	94.038	93.505
830.2237	95.801	95.612	95.301	94.934	94.462	93.944	93.411
948.8271	95.801	95.565	95.246	94.857	94.389	93.856	93.302
1067.43	95.740	95.504	95.202	94.807	94.323	93.785	93.198
1186.034	95.729	95.485	95.151	94.730	94.245	93.702	93.098
1067.43	95.785	95.539	95.213	94.819	94.307	93.767	93.164
948.827	95.831	95.605	95.278	94.879	94.378	93.839	93.252
830.224	95.889	95.713	95.350	94.955	94.471	93.921	93.339
711.62	95.949	95.746	95.427	95.021	94.532	93.993	93.433
593.0169	96.010	95.801	95.477	95.075	94.592	94.070	93.538
474.413	96.054	95.839	95.531	95.131	94.664	94.154	93.630
355.81	96.086	95.893	95.581	95.186	94.707	94.252	93.745
237.207	96.133	95.927	95.606	95.247	94.797	94.338	93.856
118.6034	96.177	95.966	95.666	95.301	94.856	94.427	93.964
0.0	96.246	96.014	95.718	95.361	94.938	94.510	94.076

TABLE 2. CONCLUDED

	Blade 4 Deflection, deg						
Rotor Azimuth	90°	105°	120°	135°	150°	165°	180°
Applied Load, ft-lb							
0.0	348.558	348.970	349.233	349.432	349.514	349.519	349.431
118.6	348.443	348.898	349.178	349.360	349.453	349.448	349.354
237.2	348.371	348.819	349.112	349.299	349.393	349.375	349.299
355.8	348.289	348.745	349.032	349.242	349.338	349.327	349.244
474.4	348.195	348.666	348.964	349.193	349.299	349.294	349.228
593.0	348.096	348.585	348.904	349.129	349.261	349.238	349.162
711.6	347.992	348.503	348.854	349.074	349.195	349.195	349.074
830.2	347.910	348.420	348.778	349.036	349.156	349.145	349.041
948.8	347.803	348.338	348.706	348.970	349.091	349.096	348.992
1067.4	347.676	348.239	348.661	348.910	349.019	349.046	348.936
1186.0	347.575	348.163	348.580	348.838	348.986	348.997	348.886
1067.4	347.635	348.217	348.635	348.920	349.047	349.080	348.942
948.8	347.712	348.294	348.687	348.981	349.113	349.140	348.992
830.2	347.800	348.377	348.766	349.041	349.201	349.178	349.046
711.6	347.886	348.442	348.838	349.113	349.255	349.234	349.096
593.0	347.907	348.525	348.898	349.162	349.297	349.283	349.126
474.4	348.074	348.591	348.964	349.220	349.338	349.326	349.233
355.8	348.179	348.682	349.047	349.266	349.365	349.388	349.283
237.2	348.283	348.744	349.089	349.332	349.426	349.459	349.276
118.6	348.403	348.844	349.156	349.376	349.475	349.497	349.310
0.0	348.518	348.936	349.248	349.453	349.530	349.541	349.404

TABLE 3. REACTIONLESS LOADING DYNAMIC ACTUATORS OFF AND LOCKED OUT

	Blade 1 Deflection, deg						
Rotor Azimuth	0°	15°	30°	45°	60°	75°	90°
Applied Load, ft-lb							
593.0	3.335	3.560	3.961	4.526	5.114	5.696	6.244
711.6	3.181	3.439	3.846	4.428	5.029	5.620	6.158
830.2	2.928	3.325	3.713	4.329	4.934	5.526	6.054
948.8	2.758	3.148	3.592	4.207	4.840	5.443	5.950
1067.4	2.582	2.936	3.450	4.114	4.748	5.349	5.845
1186.0	2.423	2.756	3.296	3.977	4.638	5.240	5.736
1067.4	2.538	2.878	3.411	4.086	4.724	5.332	5.828
948.8	2.703	3.027	3.542	4.169	4.813	5.410	5.921
830.2	2.832	3.159	3.664	4.263	4.879	5.504	6.015
711.6	3.016	3.318	3.779	4.372	4.982	5.581	6.115
593.0	3.210	3.488	3.932	4.476	5.086	5.683	6.224
474.4	--	3.648	4.065	4.597	5.185	5.783	6.328
355.8	3.587	3.831	4.241	4.696	5.290	5.889	6.443
237.2	3.768	4.004	4.383	4.839	5.395	5.992	6.555
118.6	3.966	4.169	4.548	4.965	--	6.086	6.669
0.0	4.159	4.348	4.674	5.085	5.620	6.196	6.784
118.6	4.048	4.197	4.543	4.982	5.526	6.103	6.702
237.2	3.854	4.103	4.435	4.856	5.427	6.020	6.608
355.8	3.735	3.977	4.315	4.774	5.341	5.927	6.509
474.4	3.560	3.821	4.180	4.675	5.235	5.834	6.400
593.0	3.385	3.557	4.081	4.571	5.142	5.735	6.279

TABLE 3. CONTINUED

	Blade 2 Deflection, deg						
Rotor Azimuth	270°	285°	300°	315°	330°	345°	360°
Applied Load, ft-lb							
593.0	159.996	159.472	158.983	158.637	158.351	158.242	158.264
474.4	160.092	159.560	159.071	158.730	158.473	158.414	158.472
355.8	160.203	159.664	159.168	158.846	158.627	158.588	158.654
237.2	160.307	159.767	159.291	158.967	158.763	158.763	158.840
118.6	160.417	159.851	159.401	159.097	158.917	158.912	159.005
0.0	160.532	159.944	159.494	159.186	159.055	159.093	159.214
118.6	160.461	159.881	159.435	159.131	158.967	159.009	159.109
237.2	160.373	159.796	159.346	159.022	158.851	158.840	158.945
355.8	160.263	159.692	159.241	158.890	158.682	158.681	158.762
474.4	160.159	159.593	159.120	158.785	158.555	158.489	158.560
593.0	160.054	159.495	159.027	158.659	158.417	158.304	158.401
830.2	159.839	159.395	158.923	158.523	158.254	158.142	158.203
711.6	--	159.296	158.835	158.389	158.116	157.962	158.038
948.8	159.730	159.197	158.725	158.281	157.961	157.777	157.852
1067.4	159.626	159.088	158.621	158.160	--	157.566	157.648
1186.0	159.532	159.000	158.508	158.043	157.676	157.379	157.423
1067.4	159.593	159.060	158.571	158.114	157.753	157.476	157.539
948.8	159.686	159.154	158.664	158.192	157.867	157.621	157.698
830.2	159.770	159.256	158.771	158.318	158.006	157.797	157.927
711.6	159.895	159.354	158.873	158.472	158.143	157.982	158.093
593.0	159.999	159.428	159.000	158.598	158.313	158.176	158.307

TABLE 3. CONTINUED

	Blade 3 Deflection, deg						
Rotor Azimuth	180°	195°	210°	225°	240°	255°	270°
Applied Load, ft-lb							
593.0	95.878	95.729	95.438	95.005	94.565	94.071	93.565
711.6	95.801	95.620	95.327	94.892	94.450	93.950	93.449
830.2	95.762	95.488	95.214	94.774	94.323	93.824	93.340
948.8	95.674	95.377	95.075	94.653	94.197	93.692	93.225
1067.4	95.572	95.313	94.967	94.524	94.073	93.575	93.115
1186.0	95.460	95.202	94.841	94.417	93.941	93.449	92.994
1067.4	95.543	95.276	94.927	94.490	94.026	93.535	93.085
948.8	95.612	95.356	95.011	94.581	94.125	93.643	93.169
830.2	95.729	95.466	95.103	94.699	94.240	93.745	93.266
711.6	95.817	95.559	95.230	94.807	94.356	93.857	93.373
593.0	95.916	95.653	95.339	94.933	94.482	93.978	93.483
474.4	--	95.773	95.457	95.063	94.609	94.103	93.589
355.8	96.102	95.878	95.543	95.196	94.730	94.219	93.706
237.2	96.208	95.982	95.664	95.311	94.855	94.345	93.818
118.6	96.290	96.081	95.762	95.427	--	94.483	93.944
0.0	96.367	96.180	95.889	95.548	95.110	94.608	94.048
118.6	96.284	96.115	95.828	95.477	95.032	94.529	93.966
237.2	96.219	95.988	95.721	95.384	94.933	94.424	93.872
355.8	96.089	95.872	95.597	95.262	94.814	94.310	93.768
474.4	96.004	95.780	95.499	95.123	94.702	94.191	93.660
593.0	95.911	95.757	95.361	94.993	94.570	94.069	93.554

TABLE 3. CONCLUDED

	Blade 4 Deflection, deg						
Rotor Azimuth	90°	105°	120°	135°	150°	165°	180°
Applied Load, ft-lb							
593.0	347.970	348.461	348.825	349.052	349.173	349.162	349.124
474.4	348.047	348.574	348.948	349.173	349.277	349.244	349.176
355.8	348.150	348.673	349.062	349.288	349.382	349.337	349.263
237.2	348.255	348.793	349.184	349.398	349.494	349.421	349.329
118.6	348.371	348.926	349.294	349.508	349.601	349.523	349.448
0.0	348.486	349.041	349.416	349.629	349.705	349.613	349.504
118.6	348.421	348.970	349.336	349.531	349.618	349.525	349.415
237.2	348.338	348.864	349.234	349.435	349.514	349.459	349.353
355.8	348.239	348.776	349.135	349.355	349.442	349.383	349.299
474.4	348.145	348.673	349.035	349.246	349.338	349.310	349.234
593.0	348.036	348.559	348.915	349.162	349.233	349.250	349.123
830.2	347.840	348.453	348.805	349.050	349.149	349.132	349.063
711.6	--	348.333	348.662	348.945	349.029	349.041	348.948
948.8	347.733	348.217	348.552	348.810	348.931	348.959	348.865
1067.4	347.619	348.096	348.426	348.695	--	348.898	348.788
1186	347.518	347.981	348.319	348.582	348.696	348.799	348.701
1067.4	347.579	348.052	348.398	348.668	348.793	348.872	348.778
948.8	347.662	348.135	348.487	348.767	348.893	348.964	348.849
830.2	347.751	348.223	348.586	348.86	348.981	349.025	348.893
711.6	347.849	348.329	348.689	348.942	349.080	349.102	348.985
593.0	347.936	348.467	348.788	349.052	349.173	349.178	349.048

TABLE 4. CYCLIC LOADING DYNAMIC ACTUATORS OFF AND LOCKED OUT

	Blade 1 Deflection, deg						
Rotor Azimuth	0°	15°	30°	45°	60°	75°	90°
Applied Load, ft-lb							
593.0	3.300	3.62	3.966	4.631	5.175	5.773	6.288
711.6	2.449	2.746	3.263	4.330	5.037	5.675	6.202
830.2	2.012	2.335	2.867	3.698	4.494	5.532	6.077
948.8	1.620	1.935	2.552	3.433	4.307	5.306	5.949
1067.4	1.237	1.602	2.237	3.164	4.121	5.065	5.817
1186.0	0.815	1.214	1.956	2.917	3.922	4.920	5.609
1067.4	0.992	1.383	2.093	3.043	4.026	5.004	5.773
948.8	1.301	1.67	2.329	3.215	4.152	5.114	5.883
830.2	1.671	2.005	2.620	3.439	4.334	5.240	5.993
711.6	2.060	2.379	2.933	3.686	4.532	5.383	6.125
593.0	2.810	3.028	3.443	4.124	4.811	5.567	6.251
474.4	3.634	3.896	4.267	4.729	5.291	5.784	6.394
355.8	4.061	4.276	4.587	5.015	5.493	5.993	6.526
237.2	4.466	4.643	4.913	5.282	5.687	6.158	6.660
118.6	4.825	5.006	5.236	5.529	5.892	6.312	6.793
0.0	5.202	5.358	5.541	5.782	6.090	6.476	6.937
118.6	5.022	5.191	5.383	5.659	5.988	6.389	6.847
237.2	4.719	4.906	5.164	5.471	5.843	6.265	6.742
355.8	4.389	4.56	4.850	5.235	5.674	6.130	6.617
474.4	3.990	4.231	4.565	4.993	5.488	5.988	6.493
593.0	3.593	3.879	4.252	4.720	5.284	5.828	6.356

TABLE 4. CONTINUED

	Blade 2 Deflection, deg						
Rotor Azimuth	270°	285°	300°	315°	330°	345°	360°
Applied Load, ft-lb							
593	160.087	159.620	159.175	158.819	158.566	158.383	158.472
711.6	159.983	159.461	158.939	158.369	157.638	157.452	157.489
830.2	159.851	159.313	158.412	157.742	157.281	157.026	157.086
948.8	159.719	159.071	158.225	157.539	156.962	156.657	156.686
1067.4	159.582	158.819	157.987	157.248	156.657	156.292	156.304
1186	159.454	158.659	157.800	156.983	156.311	155.915	155.926
1067.4	159.541	158.753	157.906	157.099	156.467	156.077	156.090
948.8	159.643	158.855	158.049	157.295	156.720	156.351	156.379
830.2	159.752	158.995	158.227	157.515	156.998	156.697	156.747
711.6	159.890	159.159	158.406	157.768	157.308	157.066	157.121
593	160.027	159.346	158.681	158.106	157.734	157.613	157.723
474.4	160.164	159.575	159.142	158.819	158.648	158.545	158.705
355.8	160.282	159.769	159.384	159.123	158.983	158.934	159.100
237.2	160.432	159.933	159.593	159.395	159.318	159.315	159.472
118.6	160.569	160.099	159.807	159.654	159.614	159.668	159.833
0.0	160.704	160.263	160.016	159.932	159.928	160.020	160.183
118.6	160.620	160.178	159.906	159.788	159.760	159.846	160.005
237.2	160.505	160.049	159.742	159.576	159.505	159.571	159.714
355.8	160.383	159.917	159.577	159.357	159.241	159.241	159.390
474.4	160.252	159.758	159.384	159.110	158.950	158.893	159.048
593	160.133	159.593	159.192	158.857	158.597	158.544	158.609

TABLE 4. CONTINUED

	Blade 3 Deflection, deg						
Rotor Azimuth	180°	195°	210°	225°	240°	255°	270°
Applied Load, ft-lb							
593.0	95.988	95.712	95.454	95.015	94.581	94.087	93.598
474.4	96.771	96.529	96.105	95.278	94.697	94.169	93.692
355.8	97.089	96.840	96.416	95.847	95.209	94.295	93.802
237.2	97.35	97.113	96.658	96.053	95.367	94.511	93.935
118.6	97.605	97.334	96.888	96.255	95.533	94.748	94.070
0.0	97.866	97.592	97.100	96.449	95.702	94.899	94.204
118.6	97.751	97.471	96.976	96.349	95.609	94.813	94.120
237.2	97.553	97.273	96.817	96.213	95.493	94.708	94.010
355.8	97.311	97.055	96.612	96.025	95.344	94.583	93.895
474.4	97.048	96.795	96.383	95.831	95.169	94.441	93.768
593.0	96.429	96.251	95.948	95.444	94.919	94.253	93.633
711.6	95.729	95.504	95.214	94.884	94.461	94.044	93.495
830.2	95.448	95.241	94.978	94.658	94.286	93.856	93.367
948.8	95.175	94.993	94.735	94.454	94.118	93.702	93.232
1067.4	94.951	94.740	94.504	94.257	93.928	93.561	93.095
1186.0	94.697	94.510	94.295	94.065	93.760	93.400	92.953
1067.4	94.818	94.631	94.410	94.153	93.862	93.483	93.027
948.8	95.010	94.804	94.565	94.304	93.979	93.587	93.127
830.2	95.224	95.032	94.790	94.482	94.131	93.718	93.246
711.6	95.482	95.257	94.998	94.675	94.299	93.851	93.378
593.0	95.768	95.519	95.237	94.894	94.480	94.010	93.516

TABLE 4. CONCLUDED

	Blade 4 Deflection, deg						
Rotor Azimuth	90°	105°	120°	135°	150°	165°	180°
Applied Load, ft-lb							
593.0	348.069	348.508	348.816	349.030	349.129	349.156	349.069
474.4	348.142	348.635	349.008	349.435	349.991	350.008	349.964
355.8	348.269	348.765	349.520	350.002	350.250	350.307	350.239
237.2	348.409	348.980	349.677	350.157	350.475	350.568	350.513
118.6	348.541	349.225	349.855	350.358	350.685	350.804	350.754
0.0	348.673	349.367	350.019	350.554	350.918	351.057	350.997
118.6	348.602	349.288	349.931	350.464	350.804	350.946	350.887
237.2	348.500	349.184	349.816	350.318	350.645	350.782	350.711
355.8	348.393	349.068	349.667	350.157	350.458	350.548	350.469
474.4	348.256	348.910	349.508	349.959	350.233	350.299	350.217
593.0	348.129	348.723	349.268	349.681	349.896	349.860	349.735
711.6	347.979	348.497	348.827	349.022	349.059	349.033	348.868
830.2	347.866	348.333	348.624	348.776	348.816	348.748	348.597
948.8	347.717	348.178	348.453	348.569	348.569	348.491	348.344
1067.4	347.583	348.014	348.261	348.361	348.361	348.251	348.108
1186.0	347.443	347.883	348.097	348.152	348.146	348.031	347.887
1067.4	347.509	347.948	348.179	348.261	348.250	348.135	347.981
948.8	347.618	348.057	348.305	348.415	348.421	348.310	348.157
830.2	347.729	348.173	348.437	348.580	348.613	348.536	348.376
711.6	347.847	348.305	348.612	348.772	348.827	348.772	348.607
593.0	347.971	348.464	348.769	348.975	349.101	349.025	348.931

TABLE 5. COLLECTIVE LOADING DYNAMIC ACTUATORS ACTIVE AND LOCKED OUT
WITH DITHER

	Blade 1 Deflection, deg						
Rotor Azimuth	0°	15°	30°	45°	60°	75°	90°
Applied Load, ft-lb							
0.0	4.789	4.891	5.080	5.815	5.989	6.481	6.995
118.6	4.726	4.747	4.941	5.588	5.872	6.390	6.929
237.2	4.541	4.557	4.805	5.327	5.746	6.273	6.844
355.8	--	4.347	4.613	5.198	5.570	6.164	6.754
474.4	--	4.066	4.441	5.062	5.455	6.048	6.652
593.0	3.963	3.868	4.258	4.874	5.303	5.916	6.531
711.6	3.753	3.677	4.060	4.708	5.165	5.797	6.427
830.2	3.462	3.448	3.843	4.529	5.005	5.684	6.319
948.8	3.244	3.246	3.670	4.341	4.876	5.559	6.222
1067.4	3.086	3.011	3.453	4.132	4.741	5.432	6.118
1186.0	2.915	2.761	3.266	3.965	4.586	5.314	6.027
1067.4	2.667	2.879	3.376	4.041	4.655	5.388	6.094
948.8	2.762	3.006	3.470	4.145	4.763	5.491	6.185
830.2	2.897	3.104	3.583	4.293	4.874	5.585	6.265
711.6	3.044	3.380	3.789	4.460	5.029	5.703	6.367
593.0	3.271	3.599	3.961	4.608	5.175	5.827	6.458
474.4	3.461	3.809	4.154	4.775	5.318	5.947	6.563
355.8	3.695	3.990	4.349	4.948	5.474	6.074	6.662
237.2	3.935	4.224	4.570	5.114	5.624	6.200	6.766
118.6	4.172	4.428	4.785	5.291	5.775	6.318	6.877
0.0	4.404	4.622	4.998	5.462	5.928	6.456	6.972

TABLE 5. CONTINUED

	Blade 2 Deflection, deg						
Rotor Azimuth	270°	285°	300°	315°	330°	345°	360°
Applied Load, ft-lb							
0.0	160.730	160.220	159.714	159.869	159.276	159.211	159.776
118.6	160.637	160.113	159.590	159.636	159.116	159.082	159.724
237.2	160.543	160.001	159.481	159.468	158.96	158.887	159.555
355.8	--	159.873	159.340	159.274	158.733	158.693	159.359
474.4	--	159.718	159.206	159.099	158.577	158.515	159.151
593.0	160.303	159.595	159.058	158.876	158.375	158.276	158.927
711.6	160.253	159.465	158.911	158.671	158.199	158.099	158.725
830.2	160.173	159.316	158.757	158.476	157.991	157.904	158.503
948.8	160.069	159.179	158.627	158.310	157.837	157.705	158.271
1067.4	159.946	159.039	158.473	158.121	157.647	157.488	158.064
1186.0	159.824	158.908	158.327	157.957	157.439	157.294	157.846
1067.4	159.708	158.976	158.402	158.039	157.497	157.393	157.953
948.8	159.759	159.057	158.502	158.143	157.639	157.541	158.115
830.2	159.822	159.138	158.600	158.292	157.824	157.714	158.284
711.6	159.887	159.278	158.753	158.457	158.019	157.914	158.499
593.0	159.972	159.404	158.884	158.606	158.207	158.120	158.705
474.4	160.055	159.522	159.039	158.763	158.391	158.317	158.904
355.8	160.151	159.642	159.193	158.916	158.599	158.521	159.124
237.2	160.253	159.768	159.358	159.068	158.806	158.720	159.317
118.6	160.363	159.897	159.516	159.236	158.998	158.917	159.540
0.0	160.477	160.018	159.678	159.395	159.191	159.153	159.746

TABLE 5. CONTINUED

	Blade 3 Deflection, deg						
Rotor Azimuth	180°	195°	210°	225°	240°	255°	270°
Applied Load, ft-lb							
0.0	96.371	96.114	95.802	95.439	95.034	94.600	94.363
118.6	96.199	96.037	95.738	95.448	94.952	94.506	94.290
237.2	96.121	95.977	95.660	95.471	94.873	94.421	94.195
355.8	--	95.930	95.614	95.388	94.840	94.345	94.101
474.4	--	95.936	95.546	95.298	94.752	94.254	93.996
593.0	96.153	95.869	95.511	95.240	94.685	94.179	93.901
711.6	96.146	95.801	95.451	95.141	94.619	94.097	93.801
830.2	96.124	95.749	95.418	95.074	94.567	94.010	93.695
948.8	96.077	95.676	95.350	95.011	94.480	93.925	93.593
1067.4	95.995	95.641	95.306	94.987	94.416	93.849	93.491
1186.0	95.912	95.613	95.264	94.913	94.367	93.762	93.397
1067.4	95.895	95.681	95.338	94.992	94.452	93.833	93.464
948.8	95.954	95.755	95.406	95.065	94.521	93.903	93.554
830.2	96.014	95.889	95.531	95.117	94.588	93.977	93.639
711.6	96.098	95.865	95.549	95.161	94.641	94.050	93.737
593.0	96.117	95.886	95.619	95.240	94.703	94.129	93.833
474.4	96.157	95.926	95.657	95.282	94.781	94.210	93.928
355.8	96.188	95.982	95.708	95.313	94.839	94.287	94.030
237.2	96.211	96.013	95.736	95.356	94.895	94.376	94.134
118.6	96.234	96.063	95.777	95.400	94.976	94.459	94.242
0.0	96.269	96.142	95.810	95.466	95.051	94.543	94.350

TABLE 5. CONCLUDED

	Blade 4 Deflection, deg						
Rotor Azimuth	90°	105°	120°	135°	150°	165°	180°
Applied Load, ft-lb							
0.0	348.904	349.221	349.481	349.542	349.766	349.787	349.467
118.6	348.819	349.132	349.416	349.558	349.708	349.695	349.338
237.2	348.699	349.054	349.344	349.497	349.644	349.648	349.280
355.8	--	348.976	349.287	349.478	349.623	349.601	349.236
474.4	--	348.915	349.217	349.428	349.560	349.539	349.196
593.0	348.514	348.835	349.153	349.397	349.518	349.513	349.145
711.6	348.428	348.731	349.086	349.346	349.457	349.441	349.098
830.2	348.239	348.658	349.026	349.293	349.420	349.385	349.053
948.8	348.146	348.574	348.951	349.221	349.348	349.334	349.013
1067.4	348.091	348.499	348.880	349.171	349.304	349.289	348.961
1186.0	348.026	348.420	348.819	349.091	349.273	349.227	348.923
1067.4	347.925	348.479	348.881	349.157	349.370	349.297	348.985
948.8	347.986	348.552	348.933	349.236	349.423	349.346	349.047
830.2	348.068	348.647	349.036	349.285	349.455	349.404	349.105
711.6	348.152	348.687	349.078	349.327	349.492	349.449	349.134
593.0	348.244	348.754	349.140	349.383	349.531	349.482	349.170
474.4	348.331	348.827	349.194	349.432	349.583	349.532	349.216
355.8	348.430	348.912	349.262	349.488	349.620	349.577	349.254
237.2	348.527	348.991	349.313	349.546	349.663	349.633	349.324
118.6	348.625	349.080	349.372	349.608	349.722	349.695	349.355
0.0	348.719	349.180	349.441	349.685	349.789	349.733	349.422

TABLE 6. REACTIONLESS LOADING DYNAMIC ACTUATORS ACTIVE AND LOCKED OUT WITH DITHER

	Blade 1 Deflection, deg						
Rotor Azimuth	0°	15°	30°	45°	60°	75°	90°
Applied Load, ft-lb							
593.0	3.894	4.063	4.317	4.686	5.450	5.849	6.565
711.6	3.540	3.949	4.177	4.601	5.281	5.751	6.460
830.2	3.390	3.809	4.058	4.495	5.063	5.660	6.277
948.8	3.029	3.643	3.929	4.367	4.978	5.554	6.164
1067.4	2.760	3.445	3.769	4.273	4.889	5.464	6.111
1186.0	2.591	3.296	3.606	4.166	4.849	5.369	6.038
1067.4	2.723	3.423	3.706	4.267	4.944	5.441	6.127
948.8	2.885	3.576	3.844	4.356	5.025	5.532	6.220
830.2	3.014	3.683	3.963	4.464	5.107	5.614	6.308
711.6	3.216	3.878	4.097	4.566	5.183	5.709	6.416
593.0	3.376	4.055	4.262	4.656	5.285	5.807	6.522
474.4	3.542	4.239	4.370	4.769	5.371	5.909	6.622
355.8	3.728	4.401	4.545	4.904	5.465	6.023	6.722
237.2	3.927	4.593	4.667	5.022	5.554	6.124	6.826
118.6	4.101	4.770	4.808	5.124	5.665	6.234	6.933
0.0	4.308	4.949	4.913	5.217	5.753	6.336	7.038
118.6	4.162	4.833	4.772	5.129	5.671	6.251	6.945
237.2	4.008	4.670	4.660	5.043	5.564	6.167	6.848
355.8	3.853	4.473	4.489	4.947	5.469	6.065	6.742
474.4	3.678	4.334	4.381	4.842	5.371	5.946	6.637
593.0	3.513	4.114	4.219	4.727	5.273	5.848	6.529

TABLE 6. CONTINUED

	Blade 2 Deflection, deg						
Rotor Azimuth	270°	285°	300°	315°	330°	345°	360°
Applied Load, ft-lb							
593.0	160.298	159.834	159.354	158.734	158.792	158.365	158.764
474.4	160.337	159.928	159.452	158.827	158.763	158.441	158.849
355.8	160.489	160.037	159.538	158.955	158.884	158.593	158.976
237.2	160.607	160.143	159.636	159.064	159.031	158.768	159.164
118.6	160.695	160.236	159.711	159.202	159.163	158.934	159.382
0.0	160.781	160.343	159.787	159.345	159.332	159.121	159.573
118.6	160.675	160.273	159.702	159.263	159.220	158.989	159.470
237.2	160.558	160.189	159.632	159.150	159.062	158.848	159.280
355.8	160.439	160.087	159.534	159.036	158.911	158.664	159.103
474.4	160.318	160.000	159.433	158.917	158.728	158.483	158.946
593.0	160.196	159.901	159.343	158.782	158.569	158.319	158.746
711.6	160.068	159.811	159.230	158.658	158.403	158.115	158.575
830.2	159.950	159.703	159.132	158.555	158.260	157.984	158.389
948.8	159.842	159.615	159.008	158.432	158.115	157.804	158.172
1067.4	159.739	159.517	158.883	158.293	157.971	157.639	157.994
1186.0	159.648	159.430	158.734	158.133	157.816	157.451	157.776
1067.4	159.721	159.493	158.736	158.218	157.909	157.557	157.874
948.8	159.805	159.574	158.822	158.34	158.022	157.701	158.016
830.2	159.905	159.660	158.892	158.466	158.157	157.864	158.177
711.6	160.012	159.755	159.009	158.603	158.30	158.039	158.333
593.0	160.117	159.850	159.095	158.721	158.462	158.225	158.491

TABLE 6. CONTINUED

	Blade 3 Deflection, deg						
Rotor Azimuth	180°	195°	210°	225°	240°	255°	270°
Applied Load, ft-lb							
593.0	96.009	95.790	95.612	95.177	94.755	94.226	93.850
711.6	96.038	95.682	95.542	95.053	94.669	94.064	93.749
830.2	95.983	95.563	95.424	94.929	94.645	93.939	93.639
948.8	95.947	95.467	95.292	94.821	94.505	93.816	93.588
1067.4	95.903	95.376	95.186	94.683	94.373	93.686	93.443
1186.0	95.813	95.269	95.065	94.553	94.216	93.565	93.319
1067.4	95.884	95.341	95.123	94.642	94.272	93.648	93.378
948.8	95.952	95.426	95.209	94.748	94.355	93.750	93.454
830.2	96.054	95.548	95.307	94.852	94.458	93.862	93.537
711.6	96.115	95.627	95.412	94.982	94.577	93.979	93.619
593.0	96.227	95.727	95.509	95.114	94.689	94.103	93.724
474.4	96.326	95.828	95.619	95.247	94.816	94.237	93.846
355.8	96.416	95.947	95.716	95.357	94.947	94.349	93.959
237.2	96.494	96.033	95.841	95.484	95.081	94.479	94.081
118.6	96.605	96.125	95.949	95.618	95.210	94.607	94.187
0.0	96.668	96.214	96.066	95.764	95.341	94.738	94.301
118.6	96.595	96.132	95.993	95.679	95.249	94.658	94.212
237.2	96.507	96.056	95.881	95.557	95.150	94.559	94.115
355.8	96.398	95.989	95.797	95.439	95.031	94.451	93.993
474.4	96.309	95.882	95.665	95.311	94.904	94.331	93.854
593.0	96.201	95.809	95.558	95.196	94.778	94.207	93.707

TABLE 6. CONCLUDED

	Blade 4 Deflection, deg						
Rotor Azimuth	90°	105°	120°	135°	150°	165°	180°
Applied Load, ft-lb							
593.0	348.331	348.693	349.045	349.252	349.283	349.316	349.182
474.4	348.427	348.786	349.137	349.360	349.472	349.417	349.323
355.8	348.513	348.887	349.253	349.472	349.548	349.530	349.415
237.2	348.531	349.012	349.376	349.597	349.652	349.623	349.507
118.6	348.642	349.139	349.514	349.706	349.784	349.717	349.601
0.0	348.784	349.256	349.641	349.812	349.891	349.804	349.686
118.6	348.738	349.169	349.542	349.729	349.802	349.735	349.584
237.2	348.661	349.075	349.426	349.638	349.720	349.651	349.519
355.8	348.576	348.983	349.326	349.539	349.631	349.588	349.429
474.4	348.482	348.869	349.207	349.439	349.555	349.513	349.320
593.0	348.372	348.747	349.060	349.335	349.445	349.423	349.242
711.6	348.263	348.632	348.938	349.232	349.336	349.365	349.129
830.2	348.149	348.518	348.797	349.082	349.229	349.232	349.034
948.8	348.029	348.399	348.686	348.975	349.107	349.159	348.963
1067.4	347.922	348.282	348.579	348.882	348.993	349.036	348.863
1186.0	347.813	348.161	348.466	348.793	348.897	348.971	348.779
1067.4	347.864	348.227	348.572	348.853	348.955	349.032	348.842
948.8	347.930	348.306	348.655	348.929	349.048	349.110	348.938
830.2	348.000	348.412	348.766	349.019	349.133	349.189	349.001
711.6	348.101	348.508	348.857	349.111	349.219	349.266	349.093
593.0	348.188	348.636	348.993	349.218	349.308	349.346	349.185

TABLE 7. CYCLIC LOADING DYNAMIC ACTUATORS ACTIVE AND LOCKED OUT
WITH DITHER

	Blade 1 Deflection, deg						
Rotor Azimuth	0°	15°	30°	45°	60°	75°	90°
Applied Load, ft-lb							
593.0	3.896	3.984	4.335	4.903	5.467	6.034	6.477
711.6	2.891	3.289	3.903	4.510	5.230	5.909	6.366
830.2	2.483	2.936	3.612	4.168	4.892	5.756	6.245
948.8	2.146	2.575	3.266	3.922	4.668	5.522	6.112
1067.4	1.845	2.222	3.025	3.676	4.471	5.368	5.986
1186.0	1.395	1.867	2.754	3.436	4.263	5.202	5.850
1067.4	1.557	2.051	2.940	3.577	4.365	5.298	5.946
948.8	1.859	2.349	3.206	3.751	4.516	5.414	6.053
830.2	2.185	2.663	3.480	3.968	4.702	5.542	6.175
711.6	2.555	2.978	3.796	4.187	4.831	5.694	6.292
593.0	3.173	3.462	4.212	4.500	5.045	5.886	6.428
474.4	3.945	4.229	4.968	5.083	5.374	6.082	6.562
355.8	4.317	4.588	5.289	5.314	5.617	6.246	6.695
237.2	4.687	4.942	5.613	5.556	5.849	6.408	6.829
118.6	5.042	5.283	5.907	5.807	6.069	6.569	6.961
0.0	5.393	5.605	6.197	6.047	6.266	6.730	7.102
118.6	5.178	5.380	5.994	5.888	6.148	6.624	6.998
237.2	4.846	5.085	5.695	5.670	6.001	6.501	6.899
355.8	4.521	4.769	5.391	5.428	5.831	6.367	6.767
474.4	4.148	4.411	5.099	5.183	5.650	6.222	6.639
593.0	3.752	4.045	4.724	4.910	5.452	6.070	6.513

TABLE 7. CONTINUED

	Blade 2 Deflection, deg						
Rotor Azimuth	270°	285°	300°	315°	330°	345°	360°
Applied Load, ft-lb							
593.0	160.229	159.719	159.392	158.982	158.620	158.703	158.718
711.6	160.098	159.578	159.158	158.439	157.900	157.956	157.864
830.2	159.978	159.424	158.728	158.096	157.594	157.613	157.504
948.8	159.848	159.169	158.609	157.846	157.266	157.283	157.142
1067.4	159.718	159.010	158.402	157.593	156.978	156.950	156.778
1186.0	159.586	158.854	158.224	157.351	156.677	156.599	156.441
1067.4	159.687	158.955	158.327	157.490	156.849	156.811	156.652
948.8	159.801	159.072	158.467	157.689	157.095	157.109	156.968
830.2	159.924	159.212	158.635	157.918	157.387	157.435	157.309
711.6	160.050	159.363	158.813	158.149	157.667	157.769	157.656
593.0	160.183	159.540	159.037	158.455	158.073	158.171	158.204
474.4	160.314	159.769	159.422	159.042	158.754	158.980	158.977
355.8	160.445	159.939	159.645	159.323	159.070	159.371	159.358
237.2	160.587	160.102	159.847	159.583	159.393	159.738	159.709
118.6	160.723	160.273	160.042	159.841	159.703	160.094	160.055
0.0	160.863	160.442	160.225	160.099	160.002	160.423	160.397
118.6	160.761	160.329	160.084	159.928	159.804	160.193	160.168
237.2	160.518	160.198	159.912	159.727	159.550	159.916	159.872
355.8	160.395	160.059	159.720	159.516	159.278	159.593	159.541
474.4	160.262	159.920	159.527	159.277	158.973	159.269	159.202
593.0	-	159.762	159.305	159.014	158.626	158.878	158.811

TABLE 7. CONTINUED

	Blade 3 Deflection, deg						
Rotor Azimuth	180°	195°	210°	225°	240°	255°	270°
Applied Load, ft-lb							
593.0	95.940	95.805	95.541	95.143	94.723	94.283	93.803
474.4	96.769	96.415	96.023	95.531	94.958	94.384	93.901
355.8	97.027	96.665	96.256	95.795	95.252	94.531	94.007
237.2	97.249	96.892	96.511	95.991	95.432	94.752	94.132
118.6	97.458	97.113	96.673	96.178	95.606	94.898	94.264
0.0	97.694	97.328	96.853	96.357	95.771	95.050	94.400
118.6	97.568	97.186	96.717	96.240	95.665	94.951	94.277
237.2	97.370	96.985	96.536	96.092	95.533	94.830	94.126
355.8	97.162	96.779	96.336	95.925	95.373	94.705	93.989
474.4	96.925	96.568	96.127	95.740	95.261	94.566	93.849
593.0	96.446	96.184	95.80	95.488	95.039	94.375	93.709
711.6	95.822	95.533	95.158	94.950	94.742	94.173	93.576
830.2	95.567	95.289	94.928	94.761	94.537	94.017	93.434
948.8	95.326	95.047	94.694	94.563	94.354	93.868	93.295
1067.4	95.099	94.823	94.50	94.367	94.167	93.725	93.162
1186.0	94.868	94.615	94.308	94.169	93.994	93.579	93.027
1067.4	95.005	94.755	94.451	94.290	94.099	93.678	93.118
948.8	95.198	94.940	94.660	94.439	94.211	93.793	93.223
830.2	95.394	95.155	94.873	94.615	94.352	93.925	93.344
711.6	95.636	95.388	95.096	94.801	94.504	94.065	93.461
593.0	95.915	95.676	95.379	95.008	94.665	94.211	93.593

TABLE 7. CONCLUDED

	Blade 4 Deflection, deg						
Rotor Azimuth	90°	105°	120°	135°	150°	165°	180°
Applied Load, ft-lb							
593.0	348.229	348.685	348.997	349.093	349.380	349.263	158.718
474.4	348.336	348.809	349.162	349.575	350.001	349.901	157.864
355.8	348.450	348.945	349.564	349.857	350.213	350.133	157.504
237.2	348.577	349.203	349.701	350.047	350.439	350.378	157.142
118.6	348.695	349.342	349.833	350.235	350.638	350.604	156.778
0.0	348.833	349.489	349.960	350.421	350.835	350.818	156.441
118.6	348.723	349.385	349.851	350.298	350.713	350.683	156.652
237.2	348.619	349.281	349.741	350.155	350.546	350.491	156.968
355.8	348.493	349.156	349.613	349.992	350.339	350.272	157.309
474.4	348.368	349.019	349.477	349.816	350.136	350.048	157.656
593.0	348.223	348.849	349.295	349.569	349.824	349.747	158.204
711.6	348.097	348.640	348.931	349.036	349.216	349.026	158.977
830.2	347.960	348.492	348.728	348.822	348.974	348.750	159.358
948.8	347.818	348.339	348.559	348.618	348.745	348.503	159.709
1067.4	347.682	348.184	348.395	348.425	348.525	348.277	160.055
1186.0	347.543	348.038	348.241	348.238	348.332	348.060	160.397
1067.4	347.626	348.133	348.342	348.365	348.455	348.203	160.168
948.8	347.846	348.248	348.476	348.514	348.624	348.378	159.872
830.2	347.960	348.373	348.619	348.667	348.808	348.591	159.541
711.6	348.097	348.510	348.771	348.858	349.020	348.812	159.202
593.0	-	348.658	348.957	349.072	349.279	349.087	158.811

TABLE 8. COMPARISON OF DYNAMIC ACTUATOR OFF, DYNAMIC ACTUATOR ACTIVE, AND UH-60A AIRCRAFT CONTROL SYSTEM STIFFNESS ESTIMATES, COLLECTIVE LOADING

Rotor Azimuth, deg	Dynamic Actuators Off, ft-lb/deg	Dynamic Actuator Active, ft-lb/deg	UH-60A Aircraft Measurement, 1997, ft-lb/deg
0	548	541	400
15	571	547	425
30	629	624	480
45	701	665	500
60	820	826	650
75	995	995	800
90	1212	1142	1050
105	1477	1510	1400
120	1793	1848	1750
135	2042	2129	2100
150	2236	2429	2200
165	2201	2302	2200
180	2323	2473	1850
195	2505	2345	1700
210	2027	2223	1300
225	1918	1865	1050
240	1679	1777	850
255	1404	1456	700
270	1188	1214	650
285	969	896	525
300	816	825	500
315	630	636	400
330	632	627	400
345	598	600	400
360	584	578	400

TABLE 9. COMPARISON OF DYNAMIC ACTUATOR OFF, DYNAMIC ACTUATOR ACTIVE, AND UH-60A AIRCRAFT CONTROL SYSTEM STIFFNESS ESTIMATES, REACTIONLESS LOADING

Rotor Azimuth, deg	Dynamic Actuators Off, ft-lb/deg	Dynamic Actuator Active, ft-lb/deg	UH-60A Aircraft Measurement, 1997, ft-lb/deg
0	648.24	669.32	675
15	726.32	694.0	725
30	837.69	904.56	850
45	1068.4	1093.1	1000
60	1198.1	1297.0	1150
75	1233.2	1194.9	1200
90	1140.55	1133.15	1025
105	1071.4	1031.2	990
120	1033.0	978.62	975
135	1116.7	1093.6	1075
150	1169.9	1117.2	1125
165	1460.9	1374.0	1250
180	1372.75	1266.3	1300
195	1176.9	1210.2	1200
210	1109.5	1121.4	1025
225	995.65	955.22	900
240	971.14	977.64	850
255	990.73	968.19	850
270	1118.55	1006.05	1075
285	1200.7	1259.0	1175
300	1159.2	1132.9	1175
315	967.91	966.75	950
330	808.01	739.31	850
345	652.33	685.08	700
360	643.1	650.21	675

TABLE 10. COMPARISON OF DYNAMIC ACTUATOR OFF, DYNAMIC ACTUATOR ACTIVE, AND UH-60A AIRCRAFT CONTROL SYSTEM STIFFNESS ESTIMATES, CYCLIC LOADING

Rotor Azimuth, deg	Dynamic Actuators Off, ft-lb/deg	Dynamic Actuator Active, ft-lb/deg	UH-60A Aircraft Measurement, 1997, ft-lb/deg
0	308	331	310
15	330	350	355
30	383	404	395
45	469	481	450
60	633	534	550
75	698	729	660
90	909	917	720
105	718	857	705
120	749	749	630
135	619	674	565
150	524	564	520
165	481	526	520
180	466	524	515
195	516	534	515
210	540	563	550
225	606	625	560
240	729	709	570
255	744	914	580
270	905	897	575
285	764	782	520
300	624	616	430
315	488	474	365
330	381	401	325
345	318	357	305
360	321	346	305